Kinase-interacting substrate screening is a novel method to identify kinase substrates

Mutsuki Amano,[1] Tomonari Hamaguchi,[1] Md. Hasanuzzaman Shohag,[1] Kei Kozawa,[1] Katsuhiro Kato,[1] Xinjian Zhang,[1] Yoshimitsu Yura,[1] Yoshiharu Matsuura,[2] Chikako Kataoka,[2] Tomoki Nishioka,[1] and Kozo Kaibuchi[1]

[1]Department of Cell Pharmacology, Graduate School of Medicine, Nagoya University, Showa-ku, Nagoya, Aichi 466-8550, Japan
[2]Department of Molecular Virology, Research Institute for Microbial Diseases, Osaka University, Suita, Osaka 565-0871, Japan

Protein kinases play pivotal roles in numerous cellular functions; however, the specific substrates of each protein kinase have not been fully elucidated. We have developed a novel method called kinase-interacting substrate screening (KISS). Using this method, 356 phosphorylation sites of 140 proteins were identified as candidate substrates for Rho-associated kinase (Rho-kinase/ROCK2), including known substrates. The KISS method was also applied to additional kinases, including PKA, MAPK1, CDK5, CaMK1, PAK7, PKN, LYN, and FYN, and a lot of candidate substrates and their phosphorylation sites were determined, most of which have not been reported previously. Among the candidate substrates for Rho-kinase, several functional clusters were identified, including the polarity-associated proteins, such as Scrib. We found that Scrib plays a crucial role in the regulation of subcellular contractility by assembling into a ternary complex with Rho-kinase and Shroom2 in a phosphorylation-dependent manner. We propose that the KISS method is a comprehensive and useful substrate screen for various kinases.

Introduction

Protein phosphorylation is a major and essential posttranslational modification mediating intracellular signal transduction in various cellular processes. The human genome encodes more than 500 protein kinases, which are divided into at least seven classes. A single protein kinase is generally expected to have multiple substrates/phosphorylation sites. Comprehensive screening for target substrates of specific kinases is necessary to understand the signaling networks in which the protein kinases participate. Recent phosphoproteomic approaches such as liquid chromatography tandem mass spectrometry (LC/MS/MS) combined with phosphopeptide enrichment have enabled the global analysis of dynamic phosphorylation events in the cell. For example, more than 100,000 human protein phosphorylation sites have been deposited in databases, such as PhosphoSitePlus (http://www.phosphosite.org; Hornbeck et al., 2012), which is a far greater number than had previously been predicted. However, these approaches cannot identify the kinases directly responsible for phosphorylation. Intensive substrate screen for the specific kinase have been performed using peptide/protein libraries, cellular proteins, ectopic expression system, or kinase inhibitors (Hodgson and Schröder, 2011; Palmeri et al., 2014). Prediction of phosphorylation sites in silico has been also developed vigorously (Palmeri et al., 2014). Nonetheless, it remains difficult to efficiently screen for the physiological substrates

of protein kinases, particularly uncharacterized kinases. This limitation hinders our understanding of the signal transduction of most protein kinases. Dysfunctions of protein kinases are associated with various severe pathological states including cancers, inflammation, and neurodegenerative diseases. Thus, numerous protein kinases are regarded as therapeutic targets. Several protein kinase inhibitors are presently in clinical use or in preclinical trials. Again, the difficulty to identify the substrates prohibits efficient development of drug-usable inhibitors of the protein kinases (Cohen, 2002).

Rho-associated kinase/ROCK2/ROKα (Rho-kinase) is an effector of the small GTPase Rho and is implicated in various cellular functions, including cell contraction, migration, adhesion, polarity, cytokinesis, traffic, transcription, and neurite retraction (Kaibuchi et al., 1999; Riento and Ridley, 2003; Amano et al., 2010a). Rho-kinase not only directly phosphorylates myosin light chain (MLC) but also inhibits the dephosphorylation of phosphorylated MLC by inactivating MLC phosphatase through the phosphorylation of the myosin phosphatase targeting subunit 1 (MYPT1), thereby promoting actomyosin contraction (Kaibuchi et al., 1999). Rho-kinase also phosphorylates adducin, ezrin/radixin/moesin, calponin, MARCKS, and LIM-kinase for actin filament remodeling; tau, MAP2, and CRMP-2 for microtubule depolymerization; and vimentin and neurofilament subunits for intermediate filament disassembly

(Amano et al., 2010a). Additionally, Rho-kinase phosphorylates Par3, Tiam1, and p190RhoGAP to regulate cell polarity and Rho family GTPase activities (Amano et al., 2010a). However, these substrates cannot fully account for all Rho-kinase functions.

Affinity column chromatography has been used to purify ligands for receptors and receptors for ligands. However, the isolation of the substrates of protein kinases using affinity beads coated with the protein kinases has been largely unsuccessful presumably because the affinities between the protein kinases and their substrates are lower than those between ligands and their receptors. The sensitivity of LC/MS/MS to identify the proteins has been greatly improved during the past ten years. This progress in LC/MS/MS prompted us to reevaluate affinity beads coated with protein kinases for the isolation of kinase substrates on the basis of kinase–substrate complex formation. In this study, we have developed a new method using affinity beads coated with Rho-kinase as a model kinase to identify phosphorylation reactions that occur after the formation of a kinase–substrate complex and to identify phosphorylation sites. Using this method, which we refer to as kinase-interacting substrate screening (KISS), the substrates of Rho-kinase and their phosphorylation sites were identified. The majority of the identified phosphopeptide sequences shared the consensus sequence for Rho-kinase (Amano et al., 2010a), and candidate substrates were phosphorylated by Rho-kinase in vitro. Additional kinases including PKA, MAPK1, CaMK1, CDK5, PAK7, PKN, LYN, and FYN were used as baits, and a lot of candidate substrates for each kinase were identified. Among the putative substrates for Rho-kinase, several functionally associated signaling clusters were identified. The planar cell polarity (PCP) protein Scrib was identified as a novel substrate of Rho-kinase. We found that Scrib phosphorylation plays a crucial role in the regulation of local cellular contractility by assembling into a ternary complex comprising Scrib, Rho-kinase, and Shroom2.

Results

Development of the KISS method to efficiently screen for substrates of protein kinases

As shown in Fig. 1 A, after incubation of affinity beads coated with the catalytic domain of Rho-kinase (Rho-kinase-cat) with rat brain lysate and the formation of kinase–substrate complexes, the kinase-interacting proteins were incubated with or without ATP in the presence of Mg^{2+} to permit phosphorylation. To confirm the phosphorylation of substrates in the complex, the samples were subjected to immunoblot analyses using anti–phospho-motif antibodies that recognize pSer/Thr surrounded by basic residues before tryptic digestion (Fig. 1 B). Using these antibodies, numerous bands were detected for kinase–substrate complexes in the presence of ATP, whereas few bands were detected for those in the absence of ATP. The antibody that recognizes pSX(R/K) moderately detected signals for kinase–substrate complexes in the presence of ATP. The phosphorylation of known substrates for Rho-kinase, including MYPT1, ADD1, and MLC, was confirmed in an ATP-dependent manner under the conditions (Fig. 1 C). Incubation of the kinase–substrate complexes with Rho-kinase inhibitor Y-27632 before the addition of ATP reduced the phosphorylation of ADD1 and MLC in a dose-dependent fashion but showed a minimal inhibitory effect on the MYPT1

phosphorylation, presumably because MYPT1 is among the best substrate of Rho-kinase (Fig. 1 C). We also tested the kinase dead form of Rho-kinase-cat (Rho-kinase-cat-KD) as the bait, and found considerable amounts of endogenous Rho-kinase associated with Rho-kinase-cat-KD and phosphorylated MYPT1 but not ADD1 (Fig. S1 A). Because Rho-kinase is known to form a homodimer and/or oligomer through the catalytic region (Yamaguchi et al., 2006), it is likely that the kinase-dead form of Rho-kinase is not appropriate as a negative control under the conditions (Fig. S1 A). Collectively, these results suggest that the substrates that interacted with Rho-kinase were substantially phosphorylated by Rho-kinase under these conditions.

The samples were subsequently digested with trypsin, and the phosphorylated peptides were concentrated using a titanium oxide column, followed by LC/MS/MS analysis (Fig. 1 A). A total of 356 phosphorylation sites of 140 proteins were identified as preferentially phosphorylated in the presence of ATP (Fig. 2 A). We confirmed that only a limited number of phosphopeptides were detected in GST-immobilized beads (unpublished data). The candidate phosphorylation sites are summarized in Table S3 (the detailed information about the phosphorylation sites will be available in the Kinase-associated neural phospho-signaling (KANPHOS) database: https://srpbsg01.unit.oist.jp/index.php?ml_lang=en). These proteins included known substrates for Rho-kinase, such as ADD1 (α-adducin), ARHGAP35 (p190A RhoGAP), MYL9 (myosin regulatory light chain 9), and PPP1R12A (MYPT1). Motif analysis of the phosphopeptides identified by this analysis revealed that Rho-kinase phosphorylated both Ser and Thr residues to a similar extent and that basic residues were preferentially located at the −3, −2, and −1 positions of the phosphorylation sites (Fig. 2 B). Among the candidate substrates, several functional clusters were identified, including the polarity-associated complex and the spectrin membrane cytoskeletal network (Fig. 2 C). The phosphorylation of several proteins, primarily those identified from the clusters of the polarity-associated complex and spectrin network shown in Fig. 2 C, by Rho-kinase was assayed in vitro. All of these candidate proteins, including CDC42EP4, EPB4.9, LASP1, MPP2, MYO18A, Scrib, and TWF2, were phosphorylated by Rho-kinase (Fig. 3 A). To examine whether these proteins are phosphorylated by other kinases, CaMK1 and MAPK1 were used for the in vitro kinase assay (Fig. 3 A). CaMK1 has similar phosphorylation site preference to Rho-kinase, whereas MAPK1 has different preference from it. CaMK1 efficiently phosphorylated CaMKK2; moderately phosphorylated CDC42EP2, EPB49, MYO18A, and Scrib; and hardly phosphorylated the other candidate substrates for Rho-kinase. MAPK1 efficiently phosphorylated CaMKK2, CDC42EP4, EPB49, MPP2, and Scrib; moderately phosphorylated LASP1, MYO18A, and TWF2; and hardly phosphorylated the others. CaMKK2 was detected in the CaMK1 screen, and EPB49 and MPP2 were detected in the MAPK1 screen as candidate substrates (described in the following section; Fig. 3 B and Table S3). Consistently, these proteins were efficiently phosphorylated by the respective bait kinases (Fig. 3 A). It may be noted that CaMK1 showed different substrate preference from Rho-kinase in in vitro kinase assay, whereas MAPK1 showed somewhat similar preference to Rho-kinase. However, the phosphorylation sites between Rho-kinase and MAPK1 appear to be different. Collectively, these results suggest that the KISS method effectively identified Rho-kinase substrates.
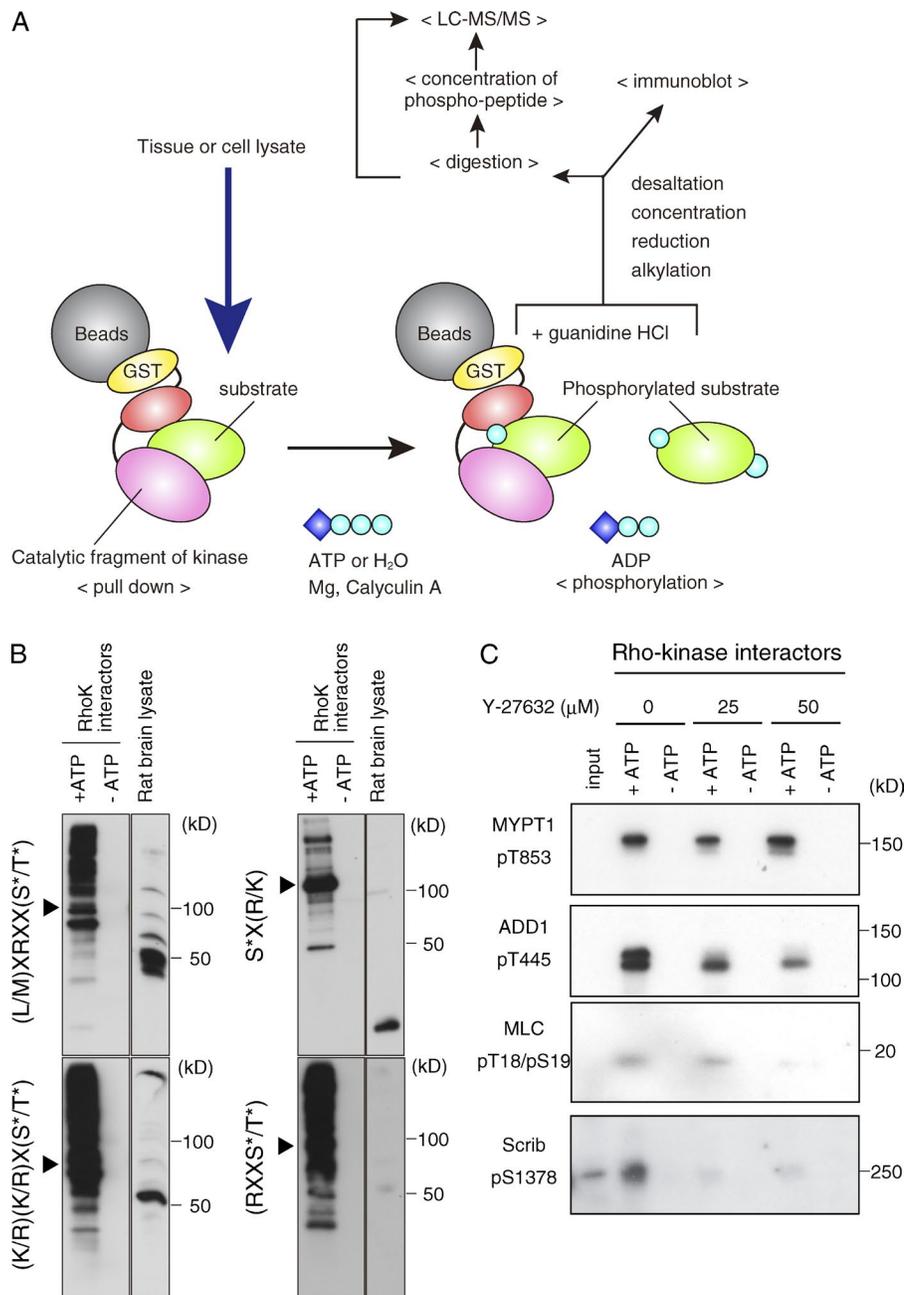
Figure 1. **Screening for Rho-kinase substrates using the KISS method.** (A) Scheme of the KISS method. (B) Detection of phosphoproteins in the KISS sample using motif-specific antibodies. GST-Rho-kinase-cat and its interacting proteins were incubated in the presence or absence of ATP to permit phosphorylation, followed by immunoblot analyses using the indicated anti–phospho-motif antibodies. Arrowheads indicate the positions of GST-Rho-kinase-cat. Several bands were detected in an ATP-dependent manner, suggesting that the interacting proteins were efficiently phosphorylated by Rho-kinase. (C) The effects of Rho-kinase inhibitor on the phosphorylation of substrates complexed with Rho-kinase. After the formation of the kinase–substrate complexes, they were treated with 25 or 50 µM of Y-27632, and then incubated in the presence or absence of ATP. The phosphorylation at MYPT1-pT853, ADD1-pT445, MLC-pT18pS19, and Scrib-pS1378 was examined by immunoblot analyses.

The KISS method is applicable to other protein kinases

To determine whether the KISS method can be extended to kinases other than Rho-kinase (AGC subfamily), the catalytic domains of PKA (AGC subfamily), MAPK1 (also known as ERK2; CMGC subfamily), CaMK1 (CAMK subfamily), CDK5 (CMGC subfamily), PAK7 (also known as PAK5; STE subfamily), PKN (AGC subfamily), LYN, and FYN (nonreceptor tyrosine kinase subfamily) were used as baits (Kondoh and Nishida, 2007; Chan and Manser, 2012; Taylor et al., 2012). We identified 422 candidate phosphorylation sites of 190 proteins for PKA, 299 sites of 103 proteins for MAPK1, 244 sites of 101 proteins for CaMK1, 184 sites of 95 proteins for CDK5, 181 sites of 97 proteins for PAK7, 206 sites of 99 proteins for PKN, 643 sites of 388 proteins for LYN, and 1062 sites of 613 proteins for FYN (Table 1). The phosphorylation sites are summarized in the Table S3. The phosphopeptide sequences identified from each kinase screen were subjected to motif analysis (Fig. 4 A). MAPK1 and CDK5 are reported to be Pro-directed kinases that require a Pro residue at the +1 position of the phosphorylation site. Consistently, Pro residues were frequently detected in the candidate phosphorylation sites for MAPK1 or CDK5 identified by this screen. PKA, CaMK1, PAK7, and PKN appeared to prefer basic residues preceding the phosphorylation sites, which is consistent with previous observations (Endicott et al., 2012). Motif analysis of the phosphopeptides identified from the LYN and FYN substrate screen exhibited a preference for phosphorylated Tyr residues surrounded by acidic residues. Because both PKA and PKN belong to AGC subfamily and have similar consensus phosphorylation sequences to Rho-kinase, the phosphopeptides detected in Rho-kinase screen are compared with those in PKA or
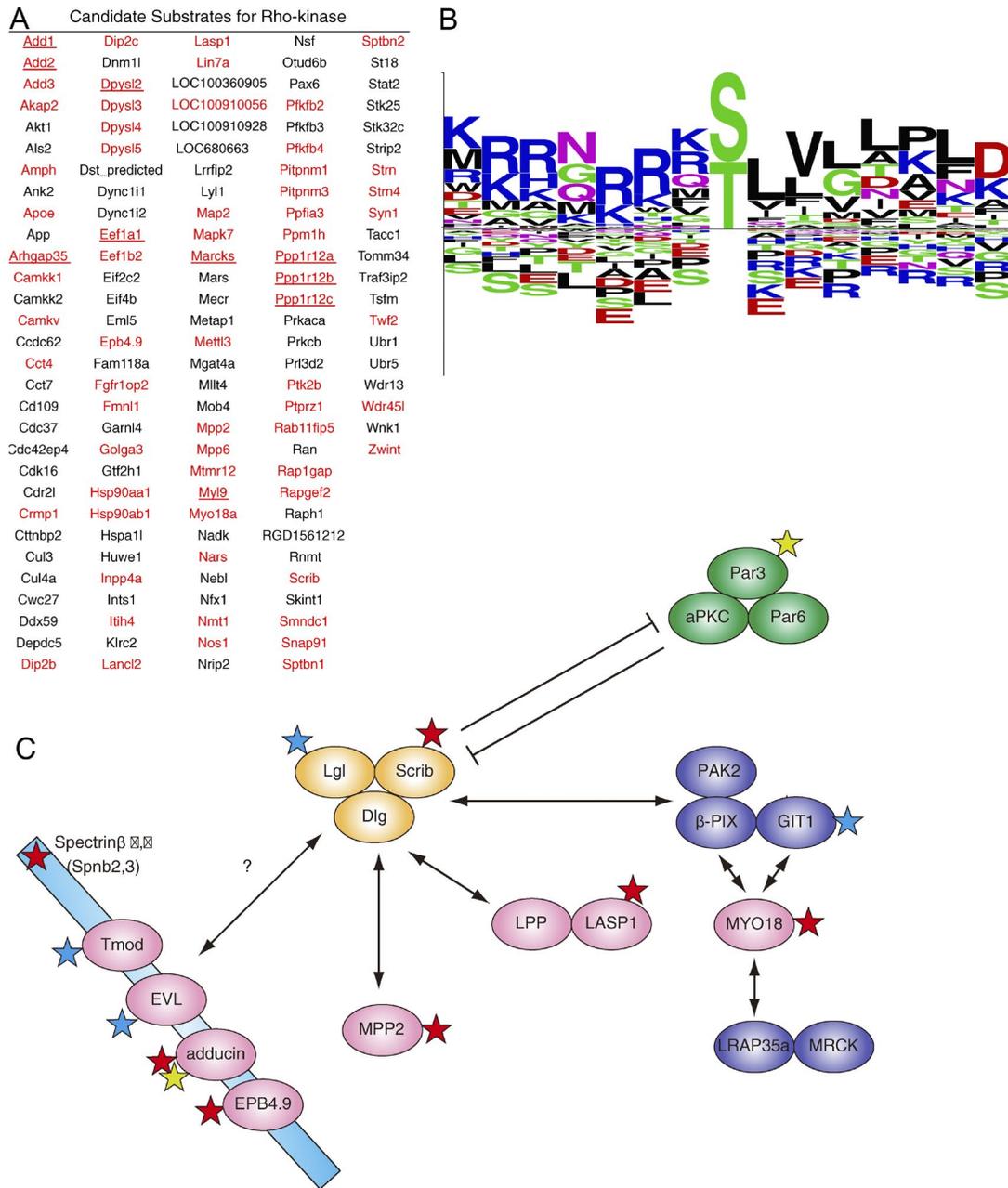
Figure 2. **The results of screen for Rho-kinase substrates.** (A) Candidate substrates determined from four independent analyses. Known substrates are underlined. Proteins that were detected twice or more times in independent analyses are indicated in red. (B) Motif logo of candidate phosphopeptides identified from the Rho-kinase screen using Logo Generators (http://www.phosphosite.org). (C) Schematic representation of the functional protein networks of Rho-kinase–interacting proteins. Red stars indicate the proteins phosphorylated by Rho-kinase identified by the KISS method; blue stars indicate the proteins identified as interacting proteins in this or a previous study (Amano et al., 2010b); and yellow stars indicate known substrates.

PKN, revealing that most of phosphorylation sites are specific for each kinase (Fig. 4 B).

Among the evaluated kinases, several substrates for PKA and MAPK1 have been identified during the past 20 yr. We found that the candidate substrates of PKA and MAPK1 included several known substrates such as GSK-3β, BRSK2, RGS14, and SYN1 for PKA and ERF, AHNAK, MKNK1, PTK2, MEF2A, and MEF2C for MAPK1 (PhosphoSitePlus). A few known substrates were identified in the candidate substrates of CaMK1, CDK5, PAK7, PKN, LYN, and FYN, possibly because of a lack of substrate information. Of interest, several Rho family guanine exchange factors (ARGHEF2,

ARHGEF7, ARHGEF11, ARHGEF12, and BCR) were identified as candidate substrates for PAK7, suggesting its function as a modulator of the Rho family signaling network. Signaling components downstream of receptor tyrosine kinases, such as SOS, RAS, PI3K, and CBL, seem to be enriched in candidate substrates for LYN and FYN.

We next wondered whether the candidate substrates were phosphorylated in vivo. More than 100,000 in vivo phosphorylation sites have been deposited in the database PhosphoSitePlus. We found that more than half of the phosphorylation sites identified by the KISS method are the registered sites by global proteomic approaches in this database, suggesting
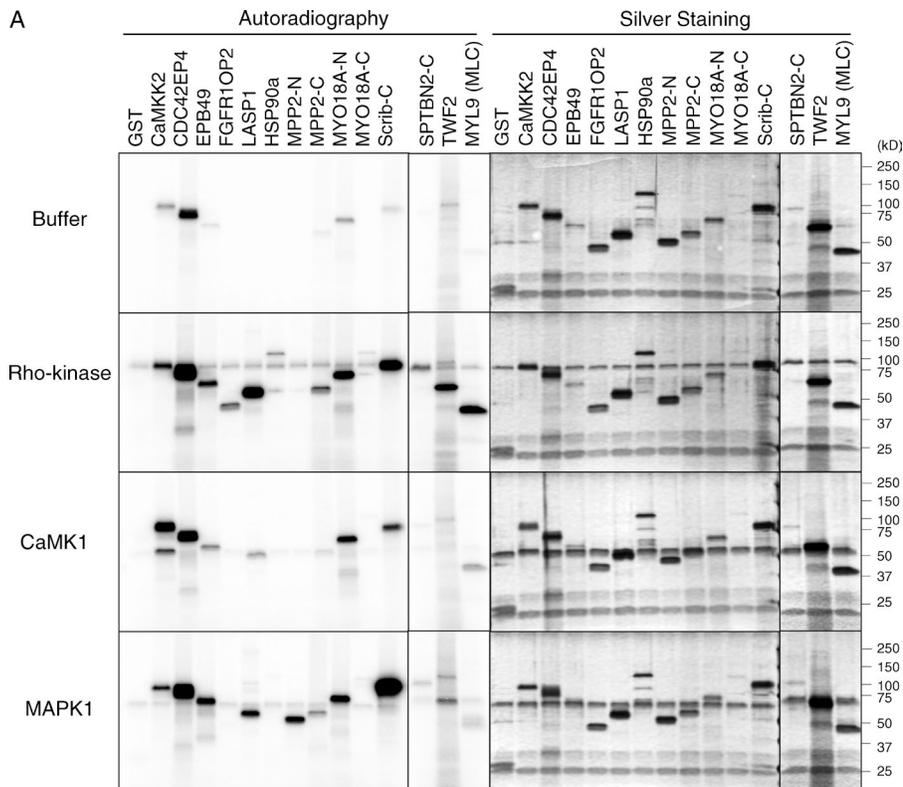
Figure 3. In vitro phosphorylation of candidate substrates. (A) Phosphorylation of candidate substrates by Rho-kinase in vitro. The recombinant candidate substrates were expressed as GST fusion proteins in COS-7 cells, pulled down with glutathione beads, and subjected to an in vitro phosphorylation assay with GST-Rho-kinase-cat, GST-CaMK1-cat, or GST-MAPK1/MEK1 in the presence of γ-[^{32}P] ATP. The reaction mixtures were subjected to SDS-PAGE analysis, and GST fusion proteins were visualized using silver staining (right). Phosphorylated proteins were imaged by autoradiography (left). (B) The phosphorylation sites for these candidate substrates detected in the screen for each kinase are summarized.

that these sites are phosphorylated in vivo, although the responsible kinase has not been determined. Additionally, the mass spectrometry results obtained using the KISS method are valuable for additional analyses, such as selected reaction monitoring and selected ion monitoring (SIM) to monitor the specific phosphorylation reaction in vivo (see the following section and Fig. S1 C).

Scrib is phosphorylated by Rho-kinase at Ser 1378 and Ser 1508 both in vitro and in vivo

Because we have extensively studied the processes of cell polarization in various cell types (Arimura and Kaibuchi, 2007; Nakayama et al., 2008; Namba et al., 2014), among the candidate substrates for Rho-kinase, we focused on Scrib to confirm whether the physiological substrate could be identified using this method. Scrib is a mammalian homologue of *Drosophila melanogaster* Scribble and has been reported to be involved in the regulation of PCP (Wansleeben and Meijlink, 2011).

Scrib is also known to be a tumor suppressor (Assémat et al., 2008; Humbert et al., 2008). Mice with a homozygous spontaneous mutation of Scrib (circletail; Crc mutant) exhibit severe failure of neural tube and eyelid closure, smaller whisker follicles (Murdoch et al., 2003), failure of cochlea kinocilium polarization (Montcouquiol et al., 2003) and wound repair (Dow et al., 2007; Caddy et al., 2010), and heart malformations (Phillips et al., 2007). Rho and Rho-kinase are also thought to play specific roles in the PCP pathway (Simons and Mlodzik, 2008); however, the underlying molecular mechanism remains largely unknown.

We were thus interested in the functional link between Scrib and Rho-kinase. Mass spectrometric analyses revealed that Ser 1387 and Ser 1516 of rat Scrib (UniProt D3ZWS0) were phosphorylated (Fig. 2 A, Fig. S1 B, and Table S3). Ser 1387 and Ser 1516 of rat Scrib correspond to Ser 1378 and Ser 1508, respectively, of human Scrib (UniProt Q14160), and hereafter, the numbering for human Scrib is used. Many phosphorylation sites including Ser 1378 and Ser 1508 have

Table 1. **Candidate substrates for the indicated kinases determined from one to three independent analyses**

Protein kinase	Candidate substrates
PKA	Adarb1, Add1,[a] Add2,[a] Add3, Agap2, Ak5, Akap2, Akap5, Aldoc, Ap2m1, Arpc2, Astn2, Atp5a1, Atp6v1b2, Atp6v1c2, Brsk1, Brsk2,[a] Ccnb3, Cct2, Cct4, Cct6a, Cct7, Cecr2, Cfl1, Ciapin1, Cog1, Cps1, Crmp1, Crym, Csrp1, Dclk1, Dgkb, Dgkz, Dmxl1, Dnm1, Dpysl2,[a] Dpysl4, Dync1i1, Eef1a1, Eef1a2, Eef2, Eif2s2, Eif4b, Eif4h, Epb41l3, Fam120a, Farp1, Farsa, Fbf1, G3bp2, Gad2, Glul, Gp1bb,[a] Gpr116, Gsk3b,[a] Habp4, Hist1h4b, Hk1, Hnrnpa1,[a] Hnrnpa2b1, Hnrnpc, Hnrnpf, Hnrnph2, Hnrnpk, Hnrnpu, Hspa12a, Idh3a, Idh3B, Ik, Il28b, Inpp5j, Itpk1, Itpka, Kcnab2, Ldhb, LOC100360057, LOC100361103, LOC680273, Map1a, Map1b, Map2,[a] Map4, Map6, Mapk1, Mapre3, Mapt,[a] Mark2, Mbp,[a] Mipol1, Mrpl3, Mthfd1, Ncan, Nfatc3, Nmt1, Nsf, Orc6, Ostm1, Pabpn1, Pacsin1, Pfkl,[a] Pfkm,[a] Pfkp,[a] Phactr1, Pkm2, Ppp1r12a,[a] Ppp1r12b, Ppp1r12c, Ppp3ca, Prkcb, Prkcg, Prpsap2, Psd3, Ptk2b, Pura, Purb, Pycrl, Ran, RGD1562399, Rgs14,[a] Rpl10l, Rpl11, Rpl13, Rpl15, Rpl17, Rpl18, Rpl18a, Rpl19, Rpl24, Rpl26-ps2, Rpl28, Rpl3, Rpl32, Rpl4, Rpl6, Rpl7, Rpl8, Rpl9, Rplp1, Rplp2, Rps10, Rps11, Rps13, Rps14, Rps15, Rps16, Rps2, Rps23, Rps24, Rps26, Rps3, Rps3a, Rps4x, Rps5, Rps6, Rps7, Rps8, Rps9, Sbds, Sept12, Sept3, Sept7, Sept8, Sept9, Sgsm1, Sik3, Skiv2l, Smarcb1, Sphkap, Srrt, Srsf2, Srsf3, Ssb,[a] Stxbp1, Syn1,[a] Syn2,[a] Syn3,[a] Tbc1d5, Tcp1, Tf, Thoc4, Tkt, Tnik, Tnr, Tppp,[a] Uba5, Ube2o, Wdr7, Zfp57, Zmym6
MAPK1	Aak1, Abhd16a, Add1, Add2, Ahnak,[a] Aldoa, Alms1, Ankrd34a, Atp5a1, Atp6v1b2, Bin1, Braf, Brsk1, Caskin1, Cdk18, Cic,[a] Crmp1, Crtc1, Crym, Dmxl2, Dnm1, Dnm1l, Dpp9, Dpysl2, Dpysl4, Dync1i1,[a] Eef1a1, Eef1d, Epb4.9, Epb41l3, Erf,[a] Gab2,[a] Garnl4, Gp1bb, Habp4, Hdac6, Hnrnph1, Hspa12a, Ints1, Irf2bp1, Irf2bpl, Itpka, Kif2a, Larp1,[a] Lmcd1, LOC685184, Lrrc47, Lysmd1, Map1a,[a] Map1b,[a] Map2,[a] Map2k2,[a] Map2k6, Map4, Mapk8ip3, Mapre3, Mapt,[a] Matr3, Mbp,[a] Mef2a,[a] Mef2c,[a] Mga, Mkl1,[a] Mknk1,[a] Mpp2, Mtx3, Napg, Nelf, Nrip2, Nsf, Pea15, Pfkp, Phactr1, Ppfia3, Ptk2,[a] Ptpdc1, Ptpn5, Rap1gap, RGD1309903, RGD1310819, Rin1, Rnf14, Rps3,[a] Rps6ka1, Rps6ka2, Sik3, Slc17a7, Smap2, Sntb1, Sos1,[a] Syn1,[a] Syn2, Synj1, Synpo, Tcp1, Tf, Tnks1bp1,[a] Tpr, Ttc9b, Ufd1l, Vom2r9, Wdr82, Wipf3
CaMK1	Add1, Add2, Add3, Amot, Amph, Ankrd34a, Apc, Araf, Arl8b, Atp6v1d, Atp6v1e1, Atxn2l, Bat2d1, Bin1, Camkk1,[a] Camkk2, Cct3, Cct4, Cetn2, Chia, Cmas, Coro7, Crmp1, Crygb, Dnm1, Dnm1l, Dpysl2, Dpysl3, Dpysl4, Eef1a1, Eef1b2, Eif4h, Elavl1, ES1 protein homolog mitochondrial, Fcho1, Fgd6, Fkbp3, Garnl3, Glrx3, Gmds, Gpr64, Gsk3b, Hcfc1, Hdac4, Hid1, Hmgcs1, Hnrnpa1, Hnrnpa2b1, Hnrnph1, Hnrnpll, Hspd1, Inpp5j, Itgb4, Kbtbd11, Kif18b, Lamc1, LOC100910056, Mab21l1, Map2, Map2k4, Map4, Map6, Mapre3, Mapt, Matr3, Mms22l, Ncoa7, Nhp2l1, Nos1,[a] Npat, Nrip2, Osbpl11, Osbpl9, Pfkl, Phactr1, Ppm1h, Prkcb, Purb, Rab18, Ralgps1, RGD1562402, Rpl3, Rps20, Rps25, Rps3a, Snca, Spire1, Sptan1, Syn1,[a] Syn2, Tcp1, Tf, Tnr, Tppp, Tpr, Ttc9, Usp4, Utp14a, Wipf3, Xirp2, Zwint
CDK5	Acsbg1, Afap1, Ahsg, Arid1a, Ash1l, Atp10a, Atp5b, Bcan, Brsk2, Camkk1, Cep57, Ckap2l, Col6a3, Crmp1,[a] Dnm1l,[a] Dync1i1, Eea1, Eef1b2, Eef2, Efcab6, Elavl1, Elavl2, Elavl4, Epb4.9, Epb41l1, Epha6, Ercc6l, Gm11639, Grm4, Gsk3a, Hnrnpa2b1, Kif14, Klhdc5, Klri2, Ldhb, LOC100360905, LOC684545, LOC689635, Map2,[a] Map7d2, Mark1, Mark2, Mt-nd5, Ncan, Nckap5l, Ncl, Npm1, Nsf, Pcdhgb8, Pfkp, Phf8, Pkm2, Plcb1, Ppp1r2,[a] Ppp3ca, Prelid1, Prkaca, Prkar2a, Prkcb, Psd3, Ptprz1, Purb, Rnf14, Rpl10l, Rpl18, Rpl23, Rpl4, Rps11, Rps14, Rps2, Rps27, Rps3, Rps7, Rps9, Rsbn1, Siglec5, Slk, Sptbn4, Srp72, Syn1,[a] Synj1,[a] Tardbp, Tert, Tf, Tgfbrap1, Thoc7, Tmprss13, Ttc37, Ufd1l, Usp7, Vps13c, Whsc2, Wipf3, Xirp2, Xkr5
PAK7	Abca4, Adcy3, Akt1, Arhgef11, Arhgef12, Arhgef2,[a] Arhgef7, Atp5a1, Atp6v1b2, Bcr, Casc4, Cct2, Cdc42ep4, Cdh20, Cdk18, Clca4, Creb3l1, Crmp1, Ctnnd2, Ddx5, Defb36, Dpysl2, Dpysl3, Dpysl4, Dpysl5, Eef1a1, Eif3b, Eif3c, Eif3d, Eif3g, Eif4b, Eif4g1, Gad2, Gatad2a, Git1, Gm11639, Gpsm1, Habp4, Hes5, Hnrnpc, Hnrnpf, Hnrnpk, Hnrnph1, Hsd17b8, Ice1, Impdh2, Kif18a, Lgals2, Lmo7, LOC100360905, LOC100362277, LOC100911677, Lpin1, Lrch2, Lrig2, Map2, Mapt, Matr3, Msh3, Muc20, Ndst3, Nsf, Nt5c2, Phactr1, Pja1, Plcb1, Ppp1r12a, Ppp1r12b, Ppp1r12c, Ppp1r3c, Prkca, Prkci, Prr15l, Prrc2b, Psd3, Psmc1, Ptprf, Rapgef2, Rbm6, RGD1562402, Rpl13, Rpl3, Rps14, Rps3, Rps3a, Sarm1, Sec16a, Slc30a6, Spe39, Srrm2, Stmn2, Sugp2, Syn2, Tbc1d10b, Tll2, Ubr5, Uncharacterized protein, Vom2r3
PKN	Acap3, Acox1, Add1, Add2, Adsl, Ahcyl2, Aldh18a1, Ankrd34a, Arf1, Atp5a1, Atp5b, Camkv, Cct2, Cdk16, Crmp1, Crym, Dcx, Dpysl2, Dpysl3, Dpysl4, Dpysl5, Eef1a1, Eef1b2, Eif4b, Enthd2, Epb4.9, Eprs, Fam40a, G3bp2, Gfap, Glrx3, Gp1bb, Gpr162, Hist1h4b, Hivep1, Hnrnpa2b1, Hnrnpu, Hspa8, Itpka, Itpkc, Kctd3, Kif3c, Klc1, LOC100360905, Map1b, Map2, Marcks,[a] Matr3, Mbp, Mtss1l, Nadk, Necab1, Nefh, Nefl, Pak7, Pdpk1, Pfkfb2, Pgm2l1, Phactr1, Phactr2, Phactr3, Pip4k2b, Plcb1, Plekha1, Ppm1h, Ppp1r12a, Ppp1r12b, Ppp4r4, Prkcb, Psd3, Rasgrp2, RGD1310819, RGD1562402, Rin1, Rltpr, Rock2, Rpl19, Rpl3, Rpl9, Rps11, Rps14, Rps16, Rps25, Rps9, Rufy3, Sardh, Sarm1, Sept11, Sept6, Sord, Stk4, Stmn1, Tfip11, Thbd, Tmem69, Ulk1, Usp24, Wdr44, Wnt9b
LYN	A1i3, Aacs, Abat, Abce1, Abr, Acadl, Acan, Aco2, Acot1, Acsbg1, Actn4, Adap1, Add1, Add2, Aes, Ak1, Ak5, Aldh6a1, Aldoa, Aldoc, Amph, Anxa11, Apba1, Api5, Apoa1, Asap1, Asna1, Asrgl1, Atg2b, Atg3, Atp2a3, Atp5a1, Atp5b, Atp5o, Atp6v1a, Atp6v1b2, Atp6v1f, Atp6v1h, Bcan, Bcr, Bin1, Bpnt1, C2cd4c, C4, Cadps, Camk2a, Camk2g, Camk4, Camkk1, Cand1, Capn2, Capzb, Cbl, Cblb, Cbr1, Cct2, Cct4, Cct5, Cct6a, Cct7, Cct8, Cdk5, Celf6, Cfl1, Ckb, Clic4, Clstn1, Cltc, Clu, Cnrip1, Cops5, Cops8, Crip2, Crmp1, Crym, Csk, Csrp1, Cst3, Cttn, Cyp2g1, Dars, Dbnl,[a] Dclk1, Dctn2, Dctn5, Dgkg, Dnah8, Dnaja1, Dnaja2, Dnajb1, Dnajb6, Dnm1, Dnm1l, Dnm2, Dnm3, Dpysl2, Dpysl4, Dpysl5, Dstn, Dtx3, Dusp3, Dync1h1, Eef1a1, Eef1a2, Eef1g, Eef2, Efhd2, Ehd1, Ehd3, Eif2b3, Eif4a1, Elavl1, Elavl2, Elavl4, Elp3, Eno1, Eno2, Epb41l1, Epb41l3, Eprs, Etfb, Evl, Farsa, Farsb, Fbl, Fbxl18, Fkbp2, Fkbp4, Gad2, Gda, Gfap, Gls, Gls2, Glul, Gnao1, Gnb2l1, Gsk3b, Hist1h4b, Hk1, Hnrnpa2b1, Hnrnpk, Hnrnpl, Hnrnpu, Hnrph1, Hpcal4, Hsp90aa1, Hsp90ab1, Hsp90b1, Hspa12a, Hspa4l, Hspa8, Hspd1, Hsph1, Hyou1, Icam5, Idh3a, Idh3B, Idh3g, Iqgap1, Itih3, Katnb1, Kbtbd11, Khdrbs1, Klc2, Kpna1, Kras, Lancl2, Ldha, Ldhb, Lgi1, Lin7a, Lmcd1, LOC100360843, LOC100360905, LOC100361103, LOC100362366, LOC100365067, LOC689899, Lonp1, Lrrc47, Lsamp, Map1, Map1b, Map2, Map6, Mapk1, Mapk10, Mapk3, Mapre1, Mapre3, Mapt, Matr3, Mbp, Mgll, Mllt4, Mpp6, Mri1, Mthfd1, Mtmr14, Naca, Nap1l4, Napa, Napb, Napg, Ncdn, Ncs1, Ndrg2, Nebl, Ngef, Nipsnap1, Nmral1, Nova1, Nsf, Nsfl1c, Nubp2, Nudt10, Ogdh, Olr834, Osbpl1a, Otub1, Oxr1, Pacsin1, Paics, Pak1, Pc, Pcmt1, Pde11a, Pdhx, Pfkm, Pfkp, Pgam1, Phactr1, Piezo2, Pigu, Pik3c2b, Pik3r1, Pik3r2, Pip4k2b, Pip5k1a, Pitpna, Pitpnm1, Pkm2, Plcb1, Plcg1, Pnck, Polr2b, Ppia, Ppm1h, Ppp1ca, Ppp1r12a, Ppp1r7, Ppp2cb, Ppp3cb, Ppt1, Prdx1, Prdx2, Prkar2a, Prkar2b, Prkcb, Prkcd,[a] Prkcg, Prune2, Psmc1, Psmc2, Psmc4, Psmc5, Psmc6, Pura, Pygb, Rab1, Rab3a, Rab7a, Ran, Ranbp3, Rap1gap, Reps2, RGD1304884, RGD1305178, RGD1308958, RGD1560691, RGD1561102, RGD1562402, RGD1563570, RGD1566136, RGD1566344, Rgnef, Rgs6, Rnf14, Rock2, Rpl10l, Rpl11, Rpl23, Rpl31l4, Rpl9, Rprd1a, Rps11, Rps14, Rps16, Rps18, Rps2, Rps21, Rps24, Rps26, Rps3, Rps3a, Rps5, Rps7, Rps8, Rtn4, Rufy3, Ruvbl2, Sar1a, Sars, Scai, Sdcbp, Sec16a, Sec31a, Sfpq, Sgip1, Sh3gl1, Sh3gl2, Sh3glb2, Sh3kbp1, Sirt2, Skap2, Slc25a31, Smad2, Smap1, Snap91, Snx1, Sos1, Sos2, Spata2L, Sptan1, Sptbn2, Srr, Stip1, Stxbp1, Sugt1, Sult4a1, Syn1, Syn2, Syn3, Synj1, Synpo, Tbc1d15, Tbc1d24, Tcea1, Tf, Thop1, Tkt, Tnik, Tnk2, Tnr, Tom1l2, Tomm34, Tpm1, Tppp, Tppp3, Trim28, Tsn, Tssc1, Ttc9b, Tufm, Ube2m, Ube2o, Ubqln2, Uck1, Upf1, Vat1, Vbp1, Vcp, Vcpip1, Vps35, Vps37b, Vps4a, Wars, Was,[a] Wasl, Wdr13, Wipf2, Ywhab, Ywhae, Ywhag, Ywhah, Ywhaq, Ywhaz, Zwint

Table 1.   **Candidate substrates for the indicated kinases determined from one to three independent analyses** *(Continued)*

Protein kinase	Candidate substrates
FYN	A1i3, Abat, Abce1, Abcf3, Abi1, Abi2, Ablim1, Ablim2, Abr, Acaca, Acadl, Acan, Aco2, Acot7, Acot9, Acsbg1, Acss2, Actn1, Actn4, Acyp1, Acyp2, Adap1, Add1, Add2,[a] Adh5, Adsl, Aes, Ahcyl2, Ahi1, Ak4, Ak5, Akap8, Aldh6a1, Aldoa, Aldoc, Amph, Anks1a, Anp32a, Anxa11, Anxa6, Ap3m2, Apba1, Api5, Apoa1, Araf, Arfgef2, Arhgap32, Arhgef2, Arl3, Arpc3, Arrb1, Asap1, Asap2, Asna1, Asns, Ass1, Ate1, Atg2b, Atg3, Atic, Atp5a1, Atp5b, Atp5o, Atp6ap2, Atp6v1a, Atp6v1b2, Atp6v1c1, Atp6v1d, Atp6v1f, Atp6v1h, Atp8b2, Atxn10, Atxn2, Atxn2l, Bcan, Bcar1, Bckdha, Bcr,[a] Bin1, Blk, Brsk1, C2cd4c, C4, Cadps, Calm1, Camk1d, Camk2a, Camk2d, Camk2g, Camk4, Camkk1, Camkk2, Camkv, Camsap2, Capza2, Caskin1, Cbl,[a] Cblb, Cbr1, Cbwd1, Ccar2, Ccdc88b, Cct3, Cct4, Cct5, Cct6a, Cct7, Cct8, Cdc37, Cdk18, Cdk5,[a] Celf6, Cep170b, Cfl1, Cfl2, Churc1, Ckb, Clasp2, Clstn1, Clstn2, Cltc, Clu, Cnksr2, Cnot1, Cnp, Cnrip1, Coasy, Col6a6, Copb2, Cops5, Coq5, Coro1c, Cpsf3, Crip2, Crmp1,[a] Crtc1, Crym, Csk, Csnk2a2, Csrp1, Cst3, Cstf2t, Ctps, Ctps2, Cttn, Cul2, Cyfip2, Cyp2g1, Dars, Dclk1, Dctn5, Ddx1, Ddx19a, Ddx39b, Ddx3x, Ddx5, Dfnb31, Dgkb, Dgkg, Dip2b, Diras2, Disp1, Dlg3, Dlgap2, Dmd, Dmxl2, Dnaja1, Dnaja2, Dnaja4, Dnajb1, Dnajb5, Dnajb6, Dnm1, Dnm1l, Dnm3, Doc2b, Dock1, Dpysl2,[a] Dpysl3,[a] Dpysl4, Dpysl5, Dstn, Dtx3, Dusp3, Dync1h1, Dynll1, Eef1a1, Eef1a2, Eef1d, Eef1g, Eef2, Efhd2, Efs, Ehd1, Ehd3, Eif2b3, Eif2b4, Eif4a1, Eif4a2, Elavl1, Elavl2, Elavl3, Elavl4, Elp3, Eno1, Eno2, Epb41l1, Epb41l3, Epha7, Eprs, ES1 protein homolog mitochondrial, Exoc8, Fahd2, Fam102a, Fam120b, Fam175b, Fam65a, Farsa, Farsb, Fasn, Fbl, Fbxl18, Fh, Fhl1, Fkbp1a, Fkbp2, Fkbp4, Fuk, Fut7, G3bp2, Gab2, Gad2, Gbas, Gfap, Gga2, Git1, Glrx3, Gls, Glul, Gmds, Gnao1, Gnb2l1, Gp1bb, Grpel1, Gsk3a, Habp4, Hap1, Hapln2, Hdhd2, Hdlbp, Hint2, Hist1h4b, Hk1, Hnrnpa0, Hnrnpa1, Hnrnpa2b1, Hnrnpf, Hnrnpk, Hnrnpl, Hnrnpm, Hnrnpu, Hnrph1, Homer1, Hpcal1, Hpcal4, Hpx, Hsp90aa1, Hsp90ab1, Hspa12a, Hspa2, Hspa4, Hspa4l, Hspa8, Hspa9, Hspd1, Hsph1, Hyou1, Iars2, Icam5, Idh2, Idh3a, Idh3B, Idh3g, Igbp1, Inpp4a, Iqsec1, Itpa, Kab, Katnb1, Kbtbd11, Khdrbs1, Khdrbs3, Klc2, Kras, Lancl2, Lasp1, Lck, Ldha, Ldhb, Lgi1, Lims1, Lin7a, Lmcd1, LOC100360843, LOC100360905, LOC100361103, LOC100362298, LOC100362366, LOC100365067, LOC100365556, LOC100909464, LOC685560, LOC689899, Lonp1, Lphn3, Lrrc47, Lsamp, Magi1, Magi2, Map1, Map1a, Map1b, Map2,[a] Map2k6, Map6, Mapk1, Mapk10, Mapk3, Mapre2, Mapre3, Mapt,[a] Mars, Mat2a, Matr3, Mbp, Mettl11a, Mink1, Mllt11, Mllt4, Mpp2, Mpp6, Mri1, Mthfd1, Mtmr7, Naa30, Naca, Nampt, Napa, Napb, Napg, Nars, Ncan, Ncdn, Nck2, Ncs1, Ndrg2, Ndufv1, Nebl, Nelf, Nell2, Nfasc, Ngef, Nipsnap1, Nisch, Nmral1, Nmt1,[a] Nploc4, Nptx1, Nras, Nrip3, Nsf, Nsfl1c, Nt5c1a, Ntng2, Nubp2, Nudt10, Nxf1, Oplah, Osbpl1a, Otub1, Pacs1, Pacsin1, Padi2, Paics, Pak1, Pank4, Pc, Pcmt1, Pdia6, Pebp1, Pfkl, Pfkm, Pfkp, Pgam1, Pgls, Phactr1, Phyhip, Pick1, Pik3c2b, Pik3ca, Pik3r1, Pik3r2, Pip4k2b, Pip5k1a, Pip5k1c, Pitpna, Pitpnm1, Pkm, Pkm2, Pnck, Polr2b, Ppia, Ppm1h, Ppp1ca, Ppp1cb, Ppp1r12a, Ppp1r7, Ppp1r9b, Ppp2cb, Ppp2r1a, Ppp3ca, Ppp6c, Ppt1, Prdx1, Prdx2, Prkar2a, Prkar2b, Prkca, Prkcb, Prkcd,[a] Prkcg, Prkch, Prune2, Psat1, Psd, Psd3, Psmc1, Psmc2, Psmc3, Psmc4, Psmc5, Pten, Ptk2, Ptk2b, Ptpn11,[a] Ptprd, Pura, Purb, Pxn,[a] Pygb, Pygl, Rab1, Rab11b, Rab21, Rab2b, Rab3a, Rab3c, Rab7a, Rabggta, Rabl2a, Ralgps1, Ran, Ranbp3, Rangap1, Rap1gap, Rapgef2, Rasgrf2, RGD1304884, RGD1562399, Rgs7, Rit2, Rnf126, Rnf14, Rock2, Rph3a, Rpl10l, Rpl11, Rpl17, Rpl23, Rpl27, Rpl27a, Rpl31l4, Rpl37a-ps1, Rpl4, Rpl9, Rprd1a, Rps11, Rps12, Rps13, Rps14, Rps16, Rps2, Rps24, Rps26, Rps27l, Rps29, Rps3, Rps3a, Rps4x, Rps6, Rps6ka5, Rps7, Rps8, Rps9, Rtcd1, Rtn3, Rufy3, Ruvbl2, Samhd1, Sar1a, Sars, Sbf1, Scai, Sec31a, Sema5b, Sfpq, Sgip1, Sh2d5, Sh3gl1, Sh3gl2, Sh3glb2, Shroom2, Sirt2, Skap2,[a] Slc25a31, Smad2, Smad4, Smap1, Smap2, Smyd3, Snap91, Snrk, Snx1, Sorbs2, Sos1, Spag1, Sparcl1, Spata2L, Spon1, Sptan1, Srpr, Srr, Stam, Stat4, Stip1, Stk25, Stxbp1, Sucla2, Sugt1, Sult4a1, Syn1, Syn2, Syn3, Syne1, Syngap1, Synpo, Tanc2, Tbc1d24, Tbc1d32, Tcea1, Tcp1, Tf, Th, Them4, Thop1, Tkt, Tmem189, Tom1l2, Tomm34, Tppp, Tppp3, Tpt1, Trappc9, Trim28, Tsn, Tssc1, Tubg2, Tufm, U2af1l4, Ube2m, Ube2n, Ube2o, Ubxn6, Uck1, Unc13a, Upf1, Usp12, Usp5, Vat1, Vcp, Vcpip1, Vps18, Vps35, Vps4a, Vps4b, Vsnl1, Wars,[a] Was, Wasl, Wdr13, Wdr48, Wdr7, Wipf2, Wrnip1, Xrn2, Ywhab, Ywhae, Ywhag, Ywhah, Ywhaq, Ywhaz, Yy1, Zwint

[a]Known substrates for each kinase.

been detected by phosphoproteomic approaches (Phospho-SitePlus), whereas only Ser 1566 (Ser 1601 in mouse Scribble isoform 3) phosphorylation was functionally analyzed; this phosphorylation modulates Scrib binding to E-Cadherin–catenin complexes but the responsible kinase remains elusive (Yoshihara et al., 2011).

To confirm direct phosphorylation, three fragments of Scrib (residues 1–581, 578–1,239, and 1,235–1,630; Fig. 5 A) were expressed as GST fusion proteins and subjected to in vitro phosphorylation analysis. The C-terminal fragment (residues 1,235–1,630) containing Ser 1378 and Ser 1508 was phosphorylated by Rho-kinase in vitro with a stoichiometry of 2.47, suggesting the presence of at least three phosphorylation sites within this region (unpublished data). Additionally, the central fragment (residues 578–1,239), which contains four PDZ domains, was phosphorylated with a stoichiometry of 1.32 (unpublished data). The phosphorylation levels of the C-terminal fragments with mutations at the phosphorylation sites, Scrib-C-1378A, Scrib-C-1508A, and Scrib-C-1378A/1508A, were ~75%, 60%, and 40%, respectively, of that of the wild-type (WT) fragment (Fig. 5 B), indicating that Ser 1378 and Ser 1508 are the major phosphorylation sites within Scrib for Rho-kinase and that additional phosphorylation sites exist. Thr 1529 was identified as an additional phosphorylation site based on a series of Ala-substituted mutants (unpublished data).

To examine the phosphorylation of Scrib by Rho-kinase in vivo, we first semiquantified the phosphorylated peptides in the cell using SIM. GST-Scrib was expressed in COS-7 cells, followed by treatment with the Rho-kinase inhibitor Y-27632 or coexpressed with Rho-kinase-cat. GST-Scrib was pulled down with glutathione Sepharose beads, digested with trypsin, and subsequently subjected to LC/MS/MS analysis. The phosphopeptide containing Ser 1378 (RVpSLVGADDLRK) and that containing Ser 1508 (MKpSLEQDALR) were reproducibly detected and confirmed by MS/MS analysis. The peak intensities of both peptides were decreased in the Y-27632–treated cells and increased in the cells coexpressing Rho-kinase-cat (Fig. S1 C), suggesting that both Ser 1378 and Ser 1508 were phosphorylated in a Rho-kinase–dependent manner.

We then produced phosphorylation-specific antibodies against phosphorylated Ser 1378 and Ser 1508. These antibodies recognized Scrib that was phosphorylated by Rho-kinase, but not nonphosphorylated Scrib (Fig. S1 D). Notably, the phosphorylation of Scrib at Ser 1378 was detected in the Rho-kinase–substrate complex in the KISS method, which was reduced by the treatment with Y-27632 (Fig. 1 C). Coexpression of the constitutively active RhoA (RhoA-L63), full-length Rho-kinase, or Rho-kinase-cat with GST-Scrib increased the level of phosphorylation of both Ser 1378 and Ser 1508 in COS-7 cells (Fig. 5 C). Inhibition of endogenous Rho-kinase activity by Y-27632 decreased the levels of phosphorylation at these sites of both ectopically expressed GST-Scrib in COS-7
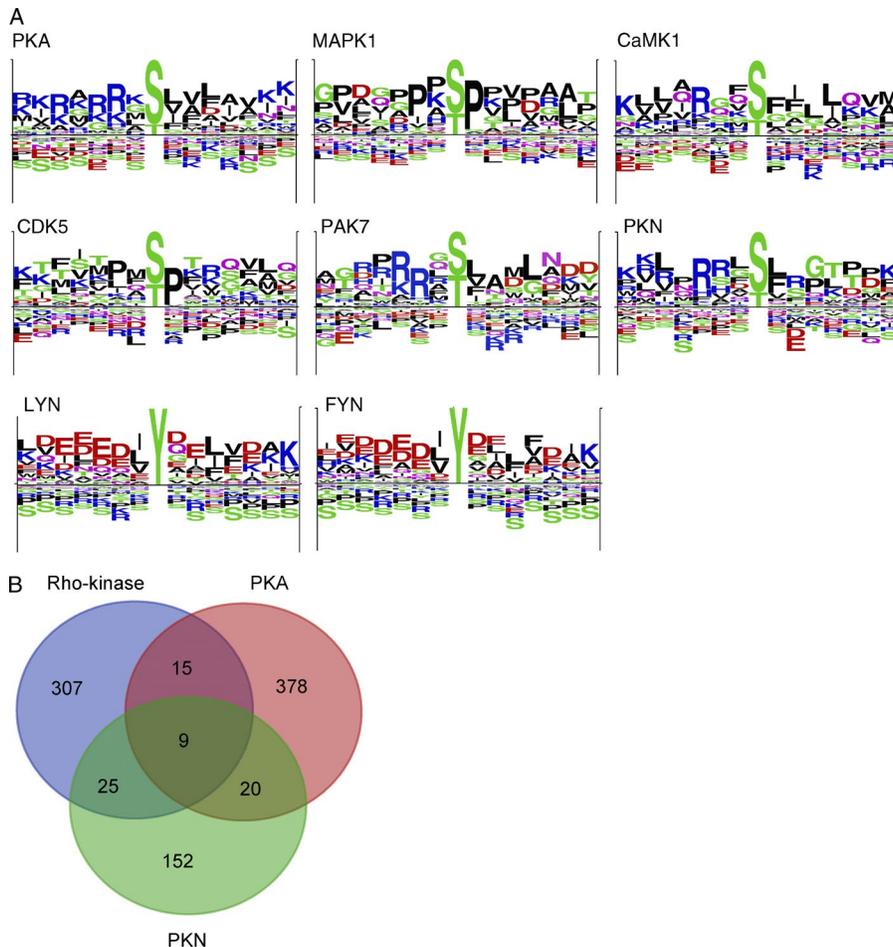
Figure 4. **Substrate screening of various kinases by the KISS approach.** (A) Motif logos of candidate phosphopeptides identified from the screens of the indicated kinases using Logo Generators. (B) Overlapping of candidate phosphorylation sites between Rho-kinase, PKA, and PKN.

cells and endogenous Scrib in MDCK II cells (Fig. 5 D). These results are consistent with mass spectrometry results and indicate that Rho-kinase phosphorylates Scrib at Ser 1378 and Ser 1508 downstream of RhoA in the cell.

Shroom2 directly binds to Scrib in a phosphorylation-dependent manner

Scrib interacts with its protein partners through 16 N-terminal leucine-rich repeats and four central PDZ domains. Scrib forms complexes with a wide variety of proteins, including Dlg, Lgl, βPIX, Vangl2, ZO2, TRIP6, LPP, and APC (Fig. 5 A; Assémat et al., 2008; Humbert et al., 2008). However, little is known regarding the functions of the C-terminal region that contains the Rho-kinase phosphorylation sites. Therefore, we searched for proteins that bind the C terminus of Scrib, particularly phosphorylation-dependent binding proteins. Phosphorylated or nonphosphorylated GST-Scrib-C was incubated with rat brain lysate and pulled down with glutathione Sepharose beads. The bound proteins were subjected to shotgun LC/MS/MS analyses, and Shroom2 and Pabpc1 were found to preferentially bind to Scrib-C that was phosphorylated by Rho-kinase compared with nonphosphorylated Scrib-C (Table S1 and Fig. S2, A and B).

Shroom2/APXL belongs to the Shroom family of proteins and has been reported to be a morphogenic protein that interacts with Rho-kinase (Lee et al., 2009; Farber et al., 2011). Shroom2 consists of an N-terminal PDZ domain and two Apx/Shroom domains (ASD1 and ASD2), which are conserved

among the Shroom family (Fig. 6 A). Rho-kinase/ROCK binds to the ASD2 domain of Shroom2 and modulates cell contractility (Farber et al., 2011); however, the regulatory mechanism of this interaction remains to be elucidated. To further determine the Scrib-binding region of Shroom2, GFP-Shroom2 fragments were coexpressed with GST-Scrib-C in COS-7 cells and pulled down with glutathione Sepharose beads. The C-terminal region (residues 978–1,616) of Shroom2 bound to Scrib (Fig. S2 C). Within the C-terminal region, the ASD2 region bound to Scrib (Fig. S2 C). We then examined whether Shroom2 directly interacts with Scrib. Purified recombinant GST-Shroom2-ASD2 and MBP-Scrib-C-WT or phosphorylation site mutants (Ser 1378, Ser 1508, and Thr 1529) were incubated in vitro, and the bound proteins were analyzed. MBP-Scrib-C-WT bound to GST-Shroom2-ASD2, and phosphorylation of Scrib by Rho-kinase enhanced this interaction (Fig. 6 B). These results indicate that the ASD2 region of Shroom2 directly interacts with the C terminus of Scrib and that this interaction is facilitated by phosphorylation. Coexpression of Rho-kinase-cat or full-length Rho-kinase in COS-7 cells increased the binding of Scrib-C to Shroom2-ASD2, whereas the Rho-kinase–specific inhibitor Y-27632 tended to decrease the binding of Scrib-C to Shroom2-ASD2 (Fig. 6 C). Active RhoA also facilitated this binding (Fig. 6 C). Although the substitution of Ser 1508 with Ala dramatically reduced the binding of Scrib-C to Shroom2-ASD2, the effect of substitution of Ser 1378 or Thr 1529 with Ala was limited (Fig. S2 D). These results suggest that Rho/Rho-kinase
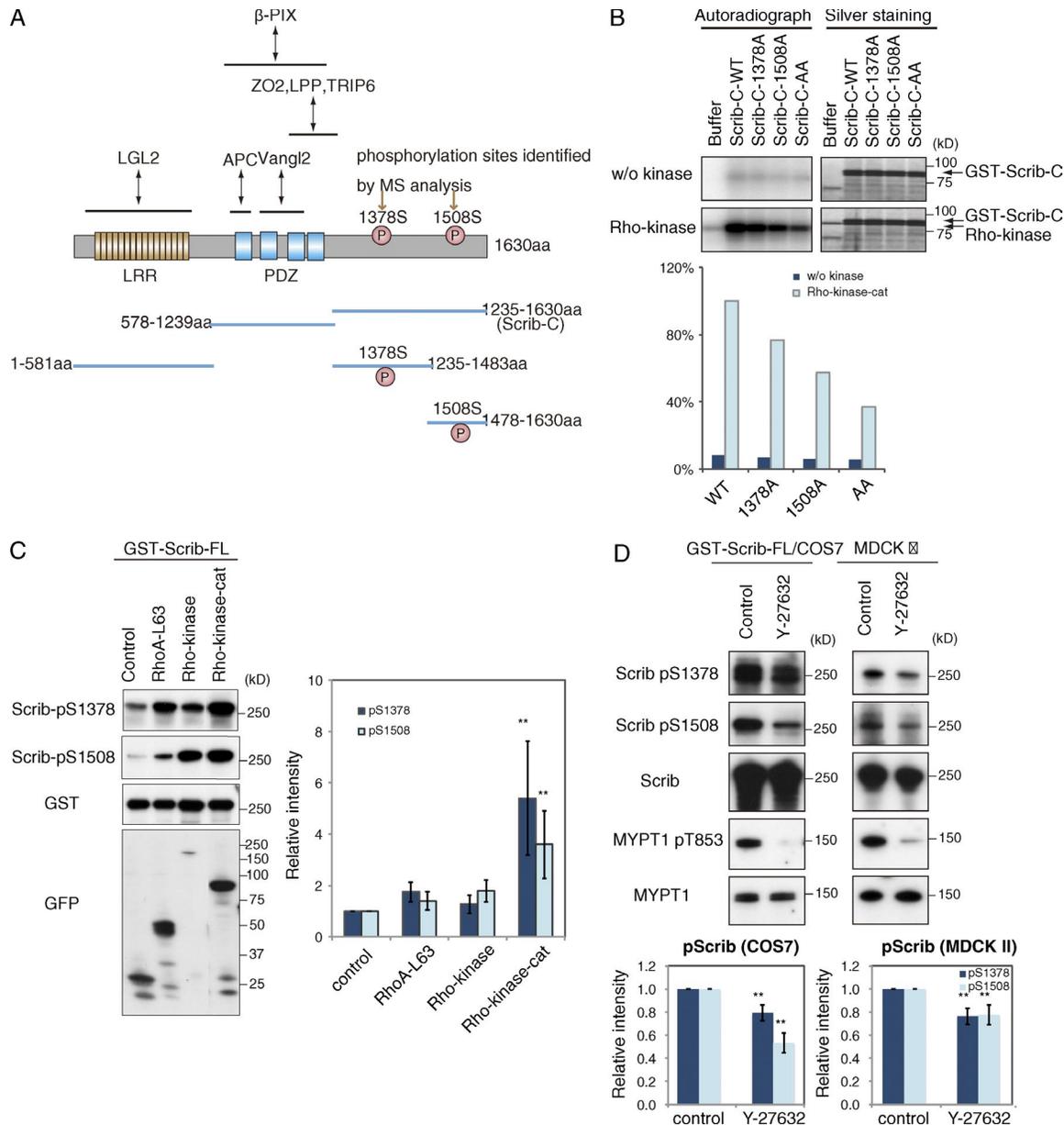
Figure 5. **Phosphorylation of Scrib by Rho-kinase.** (A) Schematic representation of the domain structure and deletion constructs of Scrib. Interacting proteins and phosphorylation sites determined by the KISS method are also indicated. (B) In vitro phosphorylation of Scrib-C (residues 1,235–1,630) and Scrib-C with mutations in the phosphorylation sites. WT and mutant GST-Scrib-C were expressed in COS-7 cells, pulled down with glutathione beads, and subjected to in vitro phosphorylation assays with or without GST-Rho-kinase-cat in the presence of γ-[^{32}P]ATP. The reaction mixtures were subjected to SDS-PAGE analysis, and GST fusion proteins were visualized using silver staining (right). Phosphorylated proteins were imaged by autoradiography (left). The data shown are from a single representative experiment out of three independent experiments. (C) Phosphorylation of Scrib in COS-7 cells. GST-Scrib and GFP-RhoA-L63, GFP-Rho-kinase, or GFP-Rho-kinase-cat was transiently expressed in COS-7 cells. The cell lysates were analyzed by immunoblot analysis using anti-pS1378 or anti-pS1508 (top two panels), anti-GST (middle), or anti-GFP antibodies (bottom). Data represent means ± SD; **, P < 0.01 as compared with control. (D) Phosphorylation of Scrib in COS-7 and MDCK II cells. COS-7 cells expressing GST-Scrib or MDCK II cells were treated with DMSO or 20 µM Y-27632 for 20 min. The cell lysates were subjected to immunoblot analysis using anti-pS1378, anti-pS1508, or anti-Scrib antibodies. Phosphorylation of MYPT1 was also examined using an anti-MYPT1 pT853 antibody. Data represent means ± SD; **, P < 0.01 as compared with control.

enhances the binding of Scrib to Shroom2 by phosphorylating Scrib primarily at Ser 1508.

We further examined whether Shroom2, Scrib, and Rho-kinase form a ternary complex in COS-7 cells and found that Shroom2 simultaneously binds Rho-kinase and Scrib in a Scrib phosphorylation–dependent manner (Fig. 7, A and B). Coexpression of both Scrib and Rho-kinase increased the binding of each protein to Shroom2 compared with Scrib and Shroom2 or Rho-kinase and Shroom2 (Fig. S2 E).

The Scrib–Shroom2–Rho-kinase complex modulates cell contractility

Focal contraction of the cell layer is controlled by both the apicobasal and the planar axes and is essential for tissue morphogenesis and wound closure (Patwari and Lee, 2008; Mammoto and Ingber, 2010; Gorfinkiel and Blanchard, 2011). Shroom2 and Shroom3 are associated with Rho-kinase (both ROCK1 and ROCK2 isoforms). This complex appears to regulate cell contraction during angiogenesis (Farber et al., 2011) and neu-

ral tube closure (Hildebrand, 2005; Nishimura and Takeichi, 2008). To clarify the role of Scrib in vivo, the localization of Rho-kinase, Scrib, and Shroom2 was examined in MDCK II epithelial cells. In a small cell colony, Scrib was localized predominantly at the cell–cell junction, as previously described (Assémat et al., 2008; Humbert et al., 2008), and it was also partially localized at the edge of the cell colony (Fig. 8 A). Rho-kinase and Shroom2 were diffusely distributed throughout the cell and discontinuously accumulated at the edge of the colony where Scrib also accumulated (Fig. 8 A). Because Rho-kinase modulates cellular contractility by regulating MLC phosphorylation (Kimura et al., 1996; Amano et al., 1996), particularly diphosphorylation (Emmert et al., 2004; Amano et al., 2010a), we also investigated the distribution of diphosphorylated MLC (ppMLC). ppMLC has been detected in various cultured cells, in certain smooth muscle tissues in response to specific agonists such as vasocontractile agents, and in pathological conditions exhibiting hypercontractility (Walsh, 2011). ppMLC was discontinuously distributed nearly exclusively at the edge of the colony, where the cell edge should be contractile, and it was marginally detected inside of the colony (Fig. 8 B). Scrib and Shroom2 were partially colocalized with ppMLC at the edge of the colony (Fig. 8 B). Similarly, Shroom2, Rho-kinase, Scrib, and ppMLC were accumulated and partially colocalized at the wound closure edge in MDCK II cells (Fig. S3).

We then examined the distribution of ectopically expressed Shroom2 in MDCK II cells. GFP-Shroom2 was discontinuously accumulated at cell–cell junctions, contractile cortical edge, and tricellular corners (Fig. 8 C). At the cortical edge, GFP-Shroom2 appeared to aberrantly recruit endogenous Scrib and Rho-kinase (Fig. 8 C), and the intensity of ppMLC staining increased (Fig. 8 E). The C terminus of Shroom2 (Shroom2-C)-Δ1428-1459aa or the Shroom2-C-Δ1433-1459aa mutant exhibited a profound loss in the ability to bind both Scrib (Fig. S4 A) and Rho-kinase (Fig. S4 B). The cortical localization of GFP-Shroom2-Δ1428-1459aa, which did not bind Scrib and Rho-kinase, was similar to that of WT; however, this mutant rarely recruited endogenous Scrib and Rho-kinase to the cortical edge in MDCK II cells (Fig. 8 C), suggesting that Shroom2 localization does not require an association with Scrib or Rho-kinase. The expression of GFP-Shroom2-Δ1428-59aa did not enhance the intensity of ppMLC staining (Fig. 8 E). The cortical localization and effects of GFP-Shroom2 on the accumulation of Rho-kinase and Scrib were perturbed by treatment with the Rho-kinase inhibitor Y-27632 (Fig. 8 D). These results suggest that Shroom2 recruits both Rho-kinase and Scrib to the cortical edge, possibly to modulate cortical contraction, and that actomyosin-driven tension at the edge is necessary for the localization of Shroom2.

We further evaluated whether the ternary complex comprising Scrib, Shroom2, and Rho-kinase is involved in cellular contraction at the cortical edge. Scrib-C-1478-1630aa, which contains Ser 1508 and Ser 1529, is the minimum fragment for binding to Shroom2 and was expected to compete with endogenous Scrib and perturb ternary complex formation. Overexpression of GFP-Scrib-C-1478-1630aa-WT resulted in a reduction of ppMLC staining at the cortical edge in the colony of MDCK II cells, whereas overexpression of Scrib-C-1478-1630aa-AA exhibited a weaker inhibitory effect (Fig. 9 A). Because depletion of Scrib exhibited negative effects on cell growth, tetracycline-inducible stable shScrib-expressing cell lines were produced (Fig. S4 C). In the cell colonies deprived of Scrib, the ppMLC staining at the cortical edge of the colony was significantly diminished (Fig. 9 B). Collectively, these results indicate that the Scrib–Shroom2–Rho-kinase complex plays a role in the regulation of the level of ppMLC and, consequently, the contractility at the cortical edge.

Discussion

Validation of the KISS approach to identifying Rho-kinase substrates

We identified 356 phosphorylation sites of 140 proteins as candidate substrates for Rho-kinase including known substrates by the KISS method. The sequence alignment of phosphopeptides is consistent with the phosphorylation consensus motif of Rho-kinase (Fig. 2 B). Among the candidate substrates, several kinases, such as AKT1, CaMKKs, CDK16, MAPK7, PKA, and STKs, were detected. Because the excess amount (500 pmol) of recombinant kinase is used as the bait and the amounts of associated protein kinases are much less than that of the bait kinase (Amano et al., 2010b), we think that the bait kinase can phosphorylate much larger amounts of peptides and that it is less likely to detect the peptides phosphorylated by associated kinases with the bait by this method. Consistently, we found that the known substrates for Rho-kinase were phosphorylated on the Rho-kinase–coated beads, and this phosphorylation was inhibited by Rho-kinase inhibitor Y-27632 (Fig. 1 C). Nonetheless, we cannot completely exclude the possibility that the identified phosphopeptides in Rho-kinase screen are phosphorylated by other kinases.

Eleven newly identified candidate substrates were subjected to in vitro phosphorylation assay, and we found that all of them were efficiently phosphorylated by Rho-kinase (Fig. 3). As for Scrib, we identified the phosphorylation sites at Ser 1378 and Ser 1508 by the KISS approaches, which were confirmed to be phosphorylated by Rho-kinase both in vitro and in vivo. We also found Thr 1529 as a phosphorylation site by Rho-kinase and unknown additional sites using the series of mutant forms of Scrib. Thr 1529 was not detected throughout the Rho-kinase substrate screen, possibly because the predicted Thr 1529–containing peptide digested by trypsin (GpTR) is too short and inappropriate for mass spectrometric analysis. Four independent analyses for Rho-kinase substrate screen do not seem to be saturated. The less abundant proteins, such as transcriptional factors and receptors, are detected stochastically by LC/MS/MS analysis. We would like to keep all information if the phosphopeptides are detected only once among the experiments. In fact, the candidate substrates (CaMKK2 and CDC42EP4), which are detected only once among four analyses, are also phosphorylated by Rho-kinase (Fig. 3).

In addition to the phosphopeptide analysis enriched with titanium oxide column, total peptide analysis without enrichment would also provide additional information. Less than 10% of Rho-kinase–binding proteins were detected in the phosphopeptide analysis, and the proteins only detected in total peptide analysis might include the substrates whose phosphopeptides are inappropriate for LC/MS/MS analysis. We consider the KISS method as a first screening and a further validation process is required to conclude whether they are physiological substrates or not by mass spectrometric information (for SIM or selected reaction monitoring) and phosphorylation site information (for preparation of mutants and antibodies).
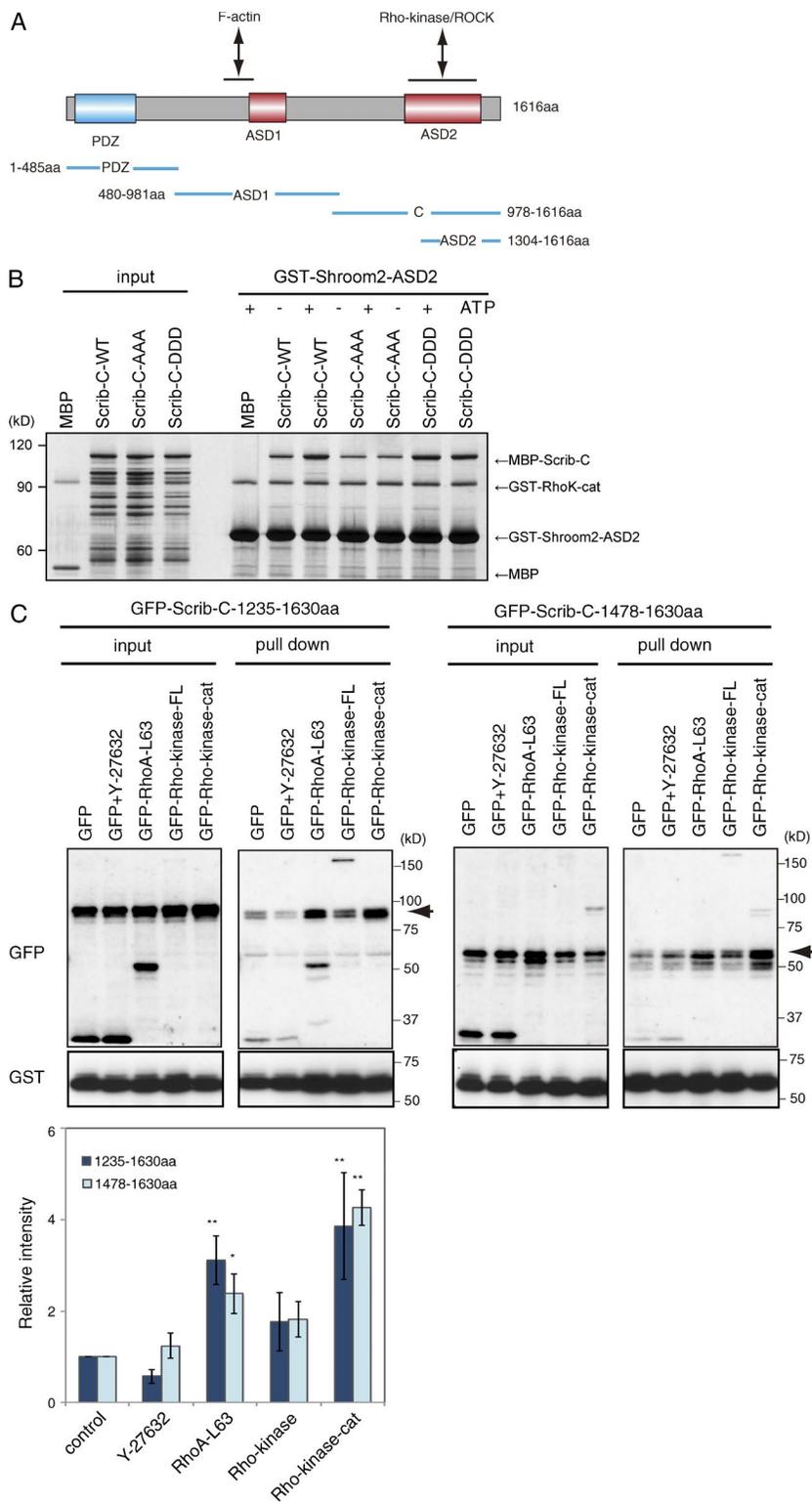
Figure 6. **Shroom2 as a novel interactor with Scrib.** (A) Schematic representation of the domain structure, constructs, and interacting proteins of Shroom2. (B) Direct interaction between Scrib and Shroom2. MBP, MBP-Scrib-C, or MBP-Scrib-C phosphorylation site mutants (S1378/S1508/T1529) were incubated with GST-Rho-kinase-cat in the presence or absence of ATP and subsequently incubated with GST-Shroom2-ASD2. GST-Shroom2-ASD2 was pulled down with glutathione beads, and the bound proteins were analyzed by silver staining. (C) Rho/Rho-kinase–dependent interaction between Scrib and Shroom2 in COS-7 cells. COS-7 cells were cotransfected with GST-Shroom2-ASD2 and GFP-Scrib-C-1235-1630aa or GFP-Scrib-C-1478-1630aa, and GST-Shroom2-ASD2 was pulled down with glutathione beads. The bound proteins were subjected to immunoblot analysis using an anti-GFP or anti-GST antibody. The Rho-kinase inhibitor Y-27632 decreased the binding of Shroom2-ASD2 to Scrib-C, whereas cotransfection with Rho-kinase-cat, Rho-kinase, or RhoA-L63 enhanced this binding. Arrows indicate the positions of GFP-Scrib-C. Data represent means ± SD; *, P < 0.05; **, P < 0.01 as compared with control.

The KISS method effectively detects substrates of various kinases and their phosphorylation sites

We evaluated the KISS method using the catalytic domains of not only Rho-kinase but also other kinases. PKN, which is also an effector of RhoA, belongs to the same AGC subfamily as Rho-kinase and exhibits the highest sequence similarity to Rho-kinase (38.1% identity and 77.4% similarity within the catalytic region) among the kinases subjected to this analysis. PKA also belongs to the AGC subfamily. MAPK1 belongs to the CMGC subfamily, CaMK1 belongs to the CAMK subfamily, and PAK7 belongs to the STE subfamily. LYN and FYN belong to the nonreceptor tyrosine kinase family. As shown in Table 1, a different subset of candidate substrates, including known substrates, were identified for each kinase. Motif analysis of the candidate sites were consistent with the preferred
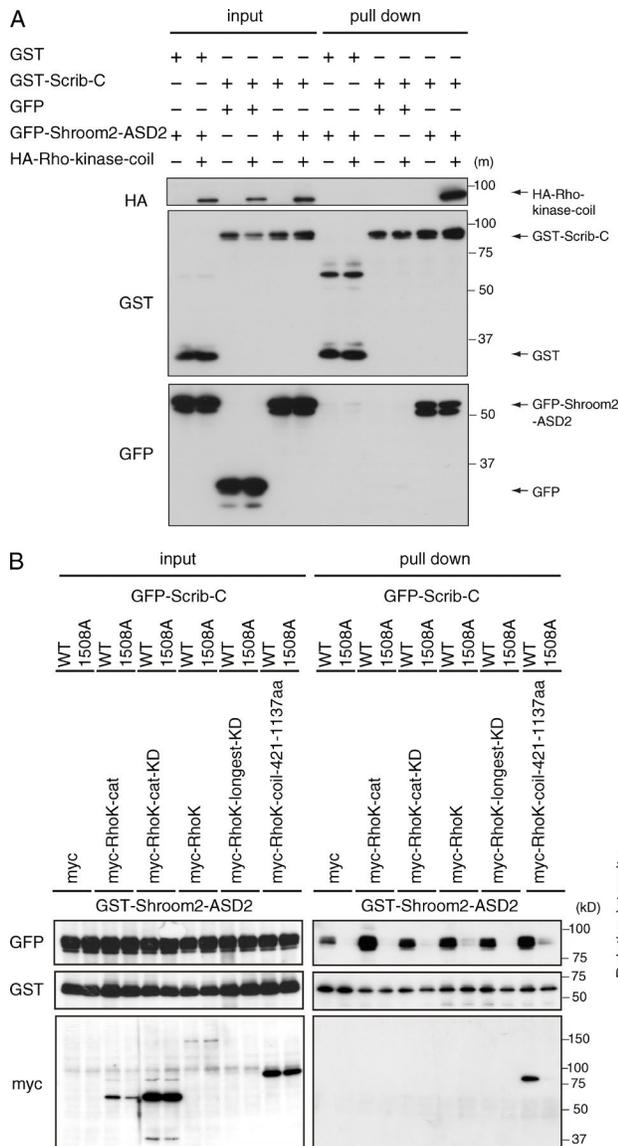
Figure 7. **Ternary complex formation between Scrib, Shroom2, and Rho-kinase.** (A) Simultaneous binding of Shroom2 to Scrib and Rho-kinase. COS-7 cells were cotransfected with GST-Scrib-C and GFP-Shroom2-ASD2 and/or HA-Rho-kinase-coil (Rho-kinase; residues 421–1,137) and pulled down with glutathione beads. The bound proteins were subjected to immunoblot analysis using an anti-GST, anti-GFP, or anti-HA antibody. Rho-kinase-coil bound to Scrib-C only in the presence of Shroom2-ASD2. (B) Enhancement of ternary complex formation by Rho-kinase. COS-7 cells were cotransfected with GST-Shroom2-ASD2, GFP-Scrib-C, and various myc-Rho-kinase fragments and pulled down with glutathione beads. The bound proteins were subjected to immunoblot analysis using an anti-GST, anti-GFP, or anti-myc antibody. Rho-kinase-coil facilitated the binding of Shroom2-ASD2 to Scrib-C as well as Rho-kinase-cat. Scrib-C-1508A failed to associate with Shroom2-ASD2 and Rho-kinase-coil. Data represent means ± SD; *, P < 0.05; **, P < 0.01 as compared with control.

sequences of the respective kinases (Fig. 4 A; Endicott et al., 2012; PhosphoSitePlus). The AGC subfamily kinases Rho-kinase, PKA, and PKN exhibit similar consensus phosphorylation sites (Figs. 2 B and 4 A) but have different candidate substrates (Fig. 2 A, Table 1, and Fig. 4 B), suggesting that the consensus sites cannot fully account for the substrate specificity of these kinases. Certain types of kinases such as MAPK1, GSK-3β, CDKs, and PDK1 have been shown to possess a docking site with the substrate that is remote from the phosphoacceptor site (Biondi and Nebreda, 2003; Goldsmith et al., 2007). A docking motif such as $(R/K)_{2–3}–X_{0–5}–\Phi–X_{1–2}–\Phi X \Phi$ (where Φ is any hydrophobic amino acid) or its inverted sequence are found in several substrates for MAPKs, and the docking interaction contributes to substrate specificity (Biondi and Nebreda, 2003; Goldsmith et al., 2007; Peti and Page, 2013). Consistently, we identified a similar docking motif in the candidate substrate for MAPK (unpublished data). Our KISS results are consistent with the rationale that kinases recognize their substrates using both phosphoacceptor and docking sites. Notably, each Ser/Thr kinase exhibits a preference for Ser or Thr as phosphorylation sites. For example, Rho-kinase phosphorylates both Ser and Thr

residues to a similar extent, whereas PKA, CaMK1, and PKN preferably phosphorylate Ser residues.

Additionally, this method provides mass spectrometric information for each phosphorylation site, which enables us to determine the intended phosphorylation levels in vivo. Indeed, we can compare the relative phosphorylation levels of Scrib at Ser 1378 and Ser 1508 in COS-7 cells based on the mass spectrometry results obtained from KISS analyses for Rho-kinase (Fig. S1 B) without the use of phosphorylation-specific antibodies. Peak intensities of both phosphopeptides were altered in a Rho-kinase activity-dependent manner in COS-7 cells (Fig. S1 C), and these results are nearly consistent with immunoblot analysis using anti-pS1378 and anti-pS1508 antibodies (Fig. 5, C and D). Thus, the KISS method demonstrates the advantage that the candidate phosphorylation sites detected in vitro are reasonably extended for validation in vivo.

The KISS method is useful to isolate functionally associated substrate clusters

Among the candidate substrates of Rho-kinase, we identified PCP proteins and membrane cytoskeletal proteins as function-
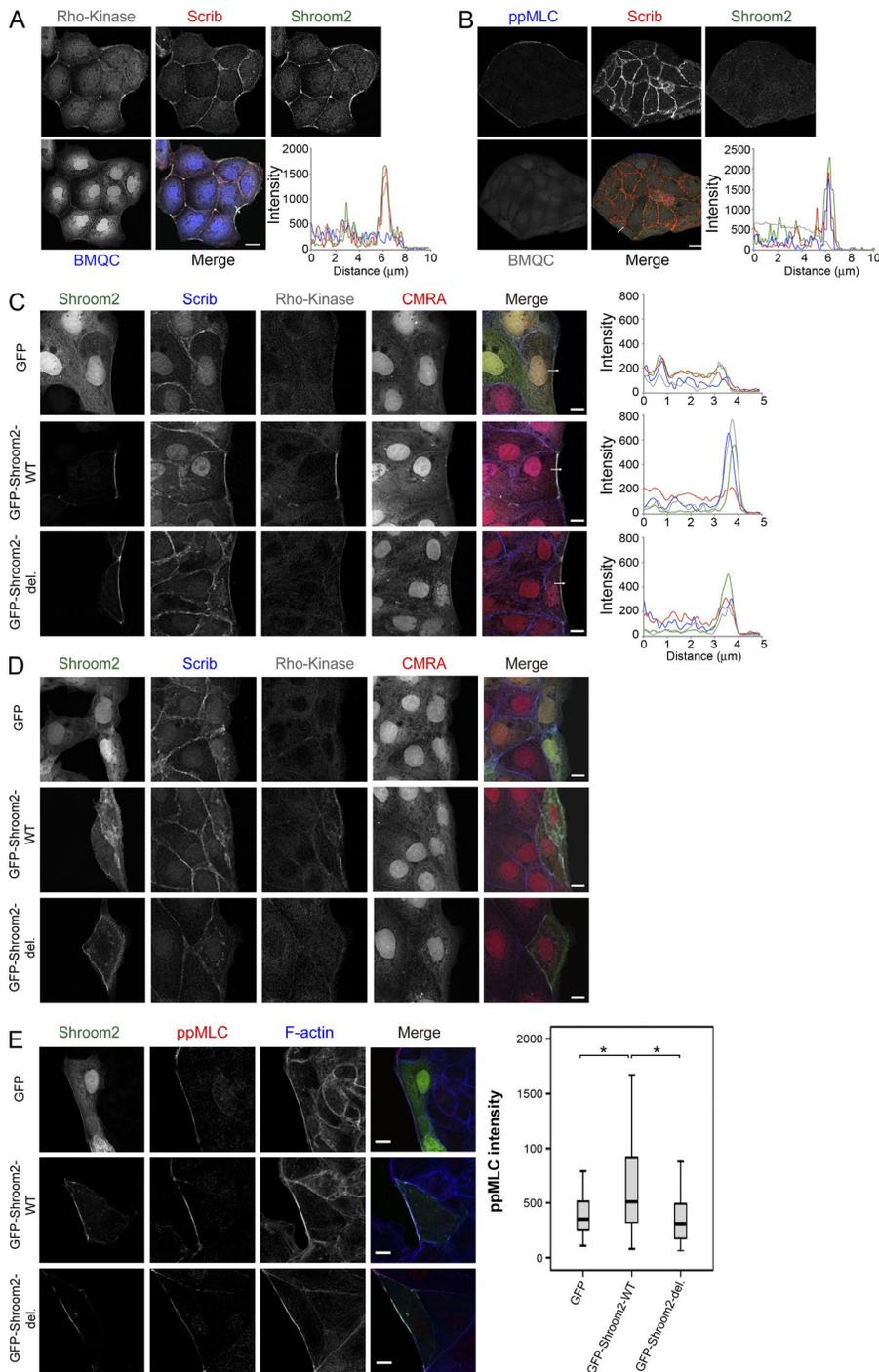
Figure 8. **Colocalization of Scrib with Shroom2, Rho-kinase, and ppMLC at the edge of a cell colony.** (A and B) Endogenous Rho-kinase (blue), Scrib (red), and Shroom2 (green; A) or ppMLC (blue), Scrib (red), and Shroom2 (green; B) were immunostained with the cytosolic marker CellTracker Violet BMQC in a colony of MDCK II cells. The intensity of each staining at the cortical edge of the cell colony indicated by arrows is shown. Bars, 20 µm. The data shown are from a single representative experiment out of at least three independent experiments. (C–E) GFP-Shroom2 or GFP-Shrom2-Δ1428-1459aa was ectopically expressed in MDCK II cells, and endogenous Scrib, Rho-kinase, and the cytoplasmic marker CellTracker Orange CMRA (C and D) or ppMLC and F-actin (E) were stained with GFP. The cells were treated with Y-27632 in D. The intensity of each staining at the cortical edge of the cell colony indicated by arrows is shown (C). The data shown are from a single representative experiment out of at least three independent experiments. The intensity of ppMLC staining at the cortical edge of the cell colony is shown (E). Bars, 10 µm. Data represent median and range with 5–95% percentiles. *, $P < 0.05$.

ally associated protein clusters (Fig. 2 C). Scrib forms a PCP complex with Dlg1 and Lgl, which is thought to antagonize the Par polarity complex (Assémat et al., 2008; Humbert et al., 2008). Scrib also binds to the βPIX–PAK–GIT1 complex, which in turn assembles with MYO18 to regulate cell migration (Audebert et al., 2004; Dow et al., 2007). MPP2 (Dlg2) has been reported to associate with Dlg1 (Karnak et al., 2002), and LPP has been reported to associate with Scrib and LASP1 (Keicher et al., 2004; Petit et al., 2005). Phosphopeptides derived from Scrib, MYO18A, MPP2, and LASP1 were detected in the Rho-kinase-cat–substrate complex incubated with ATP (Fig. 2 A and Table S3), and Lgl1 and GIT1 were also identified as Rho-kinase-cat–interacting proteins in a previous study (Amano et

al., 2010b) and in this study (unpublished data). An additional subset of proteins identified by the KISS method are membrane cytoskeleton proteins, the major components of which are α- and β-spectrin heterotetramers, ankyrin, band4.1, and adducin. These proteins form a meshwork beneath the plasma membrane that maintains the cellular shape in tissues and tethers membrane proteins (Baines, 2010). Band4.9 (EPB49/dematin) and tropomodulin are also incorporated into this meshwork (Baines, 2010). Phosphopeptides derived from spectrin β-II (SPTBN1), spectrin β-III (SPTBN2), α-adducin (ADD1), β-adducin (ADD2), and EPB49 were detected (Fig. 1 C and Table S3), and tropomodulin was identified as a Rho-kinase-cat–interacting protein (not depicted). We have previously reported that
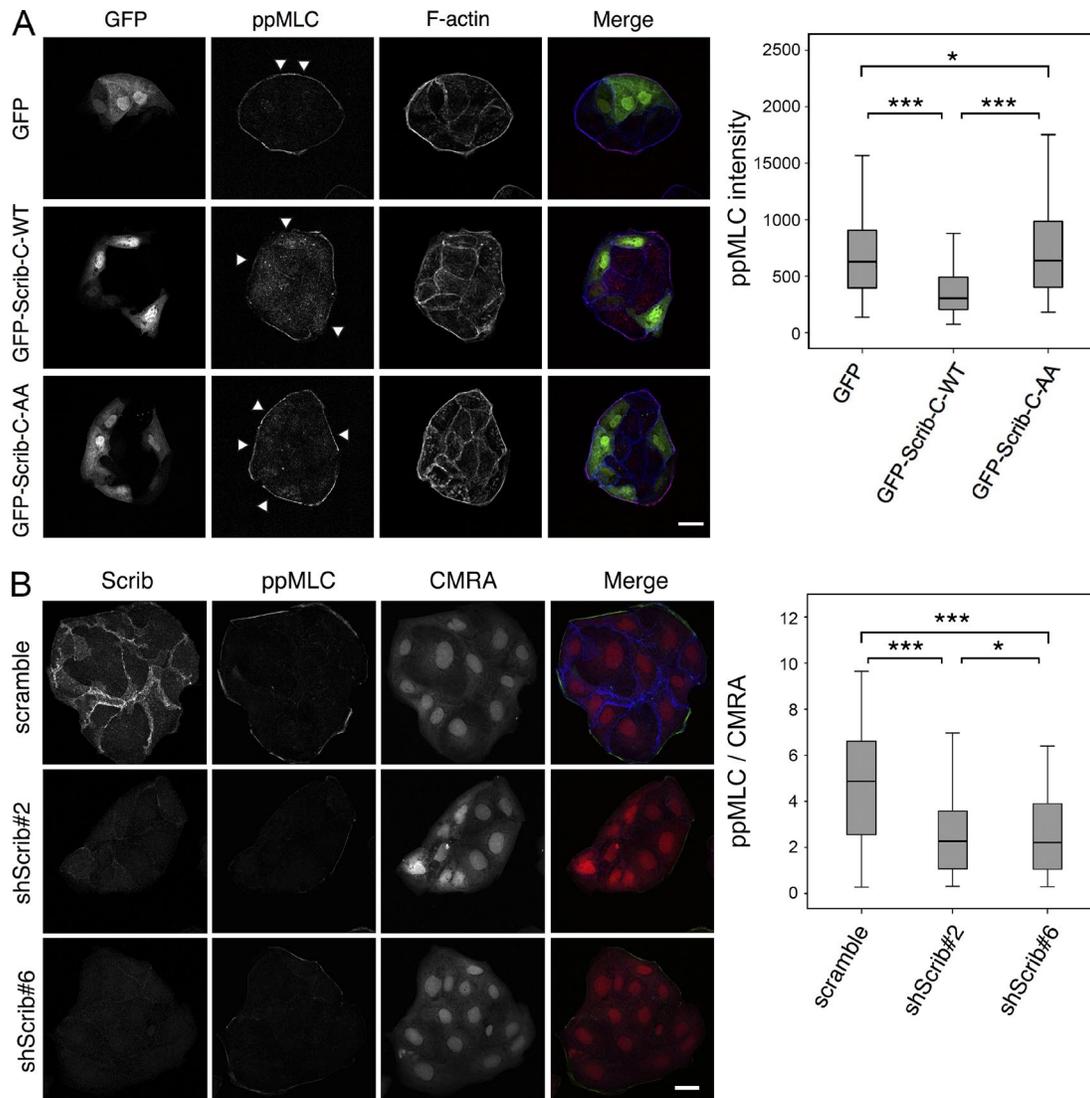
Figure 9. **Involvement of Scrib in cortical contraction.** (A) GFP-Scrib-C-WT or GFP-Scrib-C-1508A/1529A (AA) was transiently transfected into MDCK II cells, and GFP, ppMLC, and F-actin were stained. Arrowheads indicate the cells expressing GFP or GFP-Scrib-C. The intensity of ppMLC staining at the cell cortical edge of GFP- or GFP-Scrib-C–expressing cells is shown. (B) MDCK II cells stably expressing shRNA against Scrib (#2 or #6) were stained with anti-Scrib and anti-ppMLC antibodies. The intensity of ppMLC staining at the cell cortical edge of GFP- or GFP-Scrib-C–expressing cells is shown. Bars, 20 µm. Data represent median and range with 5–95% percentiles. *, $P < 0.05$; **, $P < 0.01$; ***, $P < 0.001$.

Rho-kinase phosphorylates α-adducin and modulates the association of α-adducin with F-actin (Kimura et al., 1998; Fukata et al., 1999), suggesting that Rho-kinase can directly access the spectrin meshwork in the cell. These observations may reflect the presence of the signaling cluster modulated by Rho-kinase.

The ternary complex comprising Scrib, Rho-kinase, and Shroom2 functions as a modulator of subcellular contractility

Herein, we identified Scrib as a novel substrate of Rho-kinase and found that Scrib assembles into a ternary complex with Rho-kinase and Shroom2 in a phosphorylation-dependent manner. Scrib was colocalized with Rho-kinase, Shroom2, and ppMLC at the edge of the cell colony as well as the purse string–type wound edge (free ends of plasma membranes). Overexpression of Shroom2 recruited Scrib and Rho-kinase at the edge of the cell colony. Overexpression of the C-terminal fragment of Scrib weakened the ppMLC staining at the cortical edge in a dominant-negative fashion. Similar results were obtained by reducing the expression of Scrib. These results suggest that Scrib is involved in the modulation of local contraction at the cortical edge in cooperation with Rho-kinase and Shroom2, in addition to its function at cell–cell junctions. Because Scrib-deficient mice (circletail; Crc mutant) exhibit severe failure of neural tube closure and wound repair, which reflect the impairment of apical constriction and circumferential constriction, respectively, it is quite likely that Scrib participates in these two aspects of constriction with Rho-kinase and Shroom2.

A genetic interaction between Scrib and Rho signaling has been reported in the process of wound repair after hind limb amputation in embryonic mice (Caddy et al., 2010); however, the precise underlying mechanisms remain unclear. We found the new linkage between Scrib and Rho-kinase/Shroom2 in this study, which may explain this mechanism. In our working model (Fig. 10), the upstream polarity signals, such as Wnt, activate RhoA/Rho-kinase in the tissue, and Rho-kinase
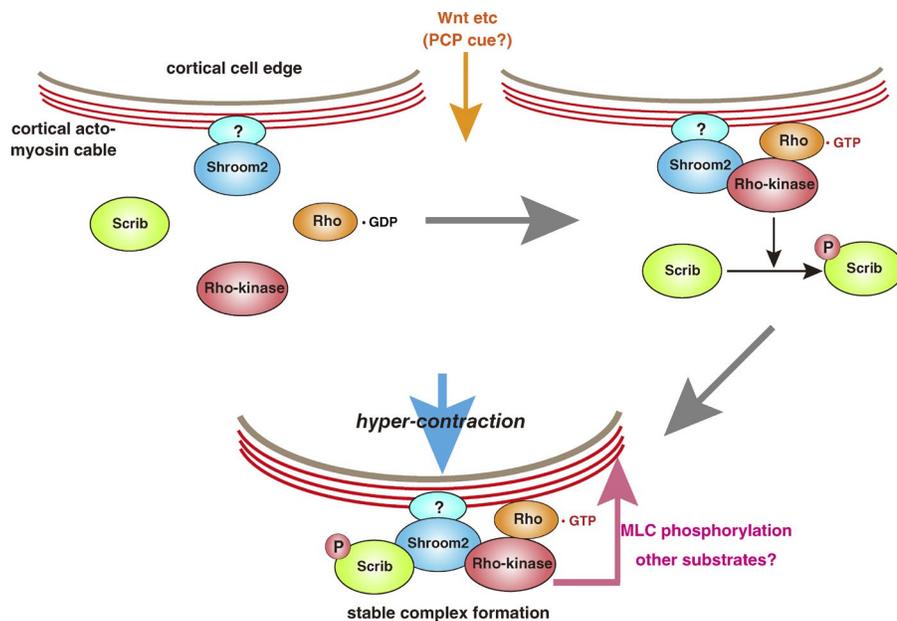
Figure 10. **Working model for local contraction modulated by Scrib–Shroom2–Rho-kinase ternary complex.**

phosphorylates Scrib and forms a stable ternary complex with Shroom2, leading to diphosphorylation of MLC and the subsequent local constriction.

Materials and methods

Materials and chemicals

Anti-(L/M)XRXX(S*/T*) (AMPK substrate) monoclonal rabbit antibody, anti-(K/R)(K/R)X(S*/T*) (PKA substrate) monoclonal rabbit antibody, anti-S*X(R/K) (PKC substrate) monoclonal rabbit antibody, anti-(RXXS*/T*) (Akt substrate) monoclonal rabbit antibody, and anti-MLC-pThr18pSer19 (ppMLC) polyclonal rabbit antibody were purchased from Cell Signaling Technology. Anti-GFP monoclonal mouse antibody (Roche), anti-Scrib polyclonal rabbit antibody (Santa Cruz Biotechnology, Inc.), anti-Scrib monoclonal mouse antibody (EMD Millipore), anti-Shroom2 polyclonal rabbit antibodies (GeneTex), and anti-MYPT1-pT853 polyclonal rabbit antibody (EMD Millipore) were purchased. CellTracker Violet BMQC and Orange CMRA were purchased from Thermo Fisher Scientific. Anti-HA monoclonal antibody (12CA5) and anti-myc monoclonal antibody (9E10) were prepared from mouse hybridoma cells. Rabbit polyclonal antibodies against Scrib phosphorylated at Ser 1378 (anti-pS1378 antibody) and Ser 1508 (anti-pS1508 antibody) were produced against the phosphopeptides PPKRVpS1378LVGAC and CARMKpS1508LEQDA, respectively. Anti-GST polyclonal rabbit antibody and anti-Adducin1-pT445 polyclonal rabbit antibody were produced against recombinant GST and phosphopeptide CQQREKpTRWLNS, respectively. Alexa 488–, Alexa 555–, and Alexa 647–conjugated secondary antibodies or phalloidin were purchased from Thermo Fisher Scientific. GST-Rho-kinase-cat (bovine, residues 6–553), GST-CaMK1α-cat (rat, residues 1–290), GST-CDK5 (human), GST-p35 (human), GST-PAK7-cat (human, residues 420–719), and GST-PKN-cat (human, residues 581–942) were expressed in Sf9 cells using a baculovirus system and purified using glutathione Sepharose beads (Amano et al., 1999). GST-PKACA and GST-MAPK1+His-MAP2K1 were provided by Y. Kirii and K. Yoshino (Carna Biosciences, Kobe, Japan). GST-Lyn and GST-Fyn were purchased from Carna Biosciences. Calyculin A and Y-27632 were purchased from Wako Pure Chemical Industries. The cDNA encoding human Scrib was provided by Kazusa DNA Research Institute (Chiba, Japan). cDNAs encoding human MPP2, MYO18A, and SPTBN2 were purchased from Promega. cDNAs encoding human Shroom2, CaM-MKK2, CDC42EP4, EPB4.9, FGFR1OP2, LASP1, Hsp90A, and TWF2 were cloned from a human brain cDNA library. cDNAs encoding full-length or fragments of Scrib, Shroom2, and other candidate substrates were cloned into pEGFP (Takara Bio Inc.), pEF-BOS-GST, pEF-BOS-myc, pEF-BOS-HA (Mizushima and Nagata, 1990), pGEX (GE Healthcare), or pMAL (New England Biolabs, Inc.) vectors. Details of all constructs used in this study are summarized in Table S2.

KISS method

Rat brain cytosolic and P2 fractions were prepared by ammonium sulfate precipitation (0–80%; Amano et al., 2000), dissolved in buffer A (20 mM Tris/HCl, pH 7.5, 1 mM EDTA, and 1 mM DTT), and incubated with glutathione Sepharose beads coated with a GST-tagged catalytic fragment of the kinase (500 pmol; Amano et al., 2010b). CDK5 exhibits low kinase activity in the absence of activators. Because kinase activity is required for the KISS method, CDK5 was copurified with p35 to obtain the active kinase to use as bait. After washing with buffer A three times, the bound proteins including kinases were incubated with (for phosphorylated samples) or without ATP/Mg^{2+} (for nonphosphorylated samples) in the 125 µl of reaction mixtures (25 mM Tris/HCl, pH 7.5, 5 mM MgCl$_2$, 1 mM EDTA, 1 mM DTT, and 0.5 µM Calyculin A). The proteins, including kinases and interacting proteins, were denatured with 7 M guanidine hydrochloride and digested with trypsin for 16 h at 37°C after reduction (4 mM DTT), alkylation (8 mM iodoacetamide), demineralization, and concentration (methanol/chloroform). The phosphopeptides were concentrated using a Titansphere Phos-TiO kit (GL Sciences) according to the manufacturer's instructions. Nanoelectrospray tandem mass analysis was performed using a Finnigan LTQ/Orbitrap mass spectrometry (for the analysis of Rho-kinase, PKA, MAPK1, CaMK1, CDK5, PAK7, and PKN) or Q Exactive mass spectrometry (for the analysis of LYN and FYN; Thermo Fisher Scientific) system combined with an HTC-PAL autosampler and a Paradigm MS4 HPLC System (Michrom BioResources Inc.) using a C$_{18}$ reversed-phase column and an ADVANCE Plug-and-Play NanoSpray Source (Michrom BioResources Inc.). A peak list was generated and calibrated using MaxQuant software (version1.3.0.5; Cox and Mann, 2008). Database searches were performed against the complete proteome set of *Rattus norvegicus* in UniProtKB (2014_07) concatenated

with reversed copies of all sequences (Peng et al., 2003). Fixed modification was set to carbamidomethylation, and variable modifications were set to phosphorylation of serine/threonine/tyrosine, oxidation of methionine, and N-terminal acetylation. Three missed cleavages by trypsin were allowed. The mass tolerance for fragment ion and the maximum peptide PEP were set to 0.5 D and 1, respectively. False discovery rates for the peptide, protein, and site levels were set to 0.01. The ion intensities of the identified peptides in the phosphorylated sample were compared with those of the nonphosphorylated sample, and the phosphorylation sites exhibiting greater than fivefold higher ion intensity were regarded as candidate substrates. Peptides containing phospho-Tyr (for Ser/Thr protein kinases) or those containing phospho-Ser/Thr (for LYN and FYN) were omitted. All kinases were analyzed at least twice.

Phosphorylation assay

Substrate proteins were expressed in *Escherichia coli* or COS-7 cells as GST or MBP fusion proteins and purified with glutathione Sepharose beads or amylose resin. The kinase reactions for Rho-kinase were performed in 50 µl of a reaction mixture (25 mM Tris-HCl, pH 7.5, 1 mM EDTA, 1 mM EGTA, 1 mM DTT, 5 mM $MgCl_2$, and 50 µM γ-[^{32}P]ATP [1–20 GBq/mmol]), GST-Rho-kinase-cat (0.01–0.1 µM), and substrates for 30 min at 30°C. The reaction mixtures were boiled in SDS sample buffer and subjected to SDS-PAGE analysis. The radiolabeled proteins were analyzed using an image analyzer (FLA9000; GE Healthcare).

Identification of proteins that interact with the C terminus of Scrib

GST-Scrib-C (residues 1,235–1,630; 500 pmol), which was expressed in *E. coli* and purified using glutathione Sepharose beads, was incubated with or without GST-Rho-kinase-cat and/or ATP/$MgCl_2$ for 30 min at 30°C and immobilized on glutathione Sepharose beads. Phosphorylated or nonphosphorylated GST-Scrib-C was incubated with rat brain lysate concentrated by ammonium sulfate precipitation (0–80%). After washing, the bound proteins were eluted with 1 M NaCl. The eluates containing 1 M NaCl and the remaining proteins on the beads were individually subjected to tryptic digestion and subsequent LC/MS/MS analyses.

In vitro binding assay

MBP, MBP-Scrib-C-WT, or MBP-Scrib-C mutants (0.5 µM) were incubated in the presence or absence of ATP in a reaction mixture (50 mM Tris-HCl, pH 7.5, 1 mM EDTA, 1 mM DTT, 5 mM $MgCl_2$, and 100 nM purified GST-Rho-kinase-cat) for 30 min at 30°C. GST-Shroom2-ASD2 (200 pmol) was immobilized onto glutathione Sepharose beads and incubated with MBP, MBP-Scrib-C-WT, or MBP-Scrib-C mutants (0.01 µM) in buffer A (20 mM Tris-HCl, pH 7.5, 1 mM EDTA, and 1 mM DTT) containing 100 mM NaCl, 0.5% NP-40, and 1 mg/ml BSA for 1 h at 4°C. The beads were washed five times with buffer A containing 100 mM NaCl and 0.5% NP-40 and then suspended in SDS-PAGE sample buffer. The bound proteins were subjected to SDS-PAGE analysis and detected by silver staining.

Cell culture

COS-7 cells were seeded on a 6-well dish at a density of 1.8×10^5 cells/well in DMEM with 10% fetal bovine serum at 37°C in an air/5% CO_2 atmosphere at constant humidity. MDCK II cells were cultured in DMEM with 10% calf serum at 37°C in an air/5% CO_2 atmosphere at constant humidity. Transfections were performed using the Lipofectamine 2000 reagent (Thermo Fisher Scientific) according to the manufacturer's protocol. For shRNA knockdown, the following complementary set of single-stranded oligonucleotides was synthesized coding Scrib target shRNAs: shScrib #2, 5′-GCACTTCAAGATCTC-

CAAG-3′ (nucleotides 1,836–1,854); and shScrib #6, 5′-GCAAC-GAGCTGGAAGTACT-3′ (nucleotides 539–557). The selected sequences were submitted to a BLAST search against the *canis lupus familiaris* genome to ensure that only the Scrib gene was targeted. To produce retroviral supernatants, GP2-293 packaging cells were transfected with 24 µg of control or Scrib shRNA-containing pSUPER-retro-puro vector and 4 µg of pVSVG using Lipofectamine 2000 reagent in collagen-coated 100-mm cell culture dishes containing Opti-MEM (Thermo Fisher Scientific). The medium was replaced 24 h later, and virus-containing supernatants were harvested 48 h after transfection and used for subsequent infection of MDCK II cells. Selection was performed using 2 µg/ml puromycin 2 d after infection.

Pull-down assay

Glutathione Sepharose beads were incubated with COS-7 cell lysates transfected with the indicated plasmids in lysis buffer (20 mM Tris-HCl, pH 7.5, 1 mM EDTA, 1 mM DTT, 150 mM NaCl, 20 mM β-glycerophosphate, 20 mM NaF, 1% NP-40, 0.1 mM APMSF, 0.5 µg/ml aprotinin, and 2 µg/ml leupeptin) for 1 h at 4°C, and the beads were subsequently washed three times with lysis buffer. After washing, the beads were resuspended with SDS-PAGE sample buffer, and the bound proteins were subjected to immunoblot analysis using the indicated antibodies.

Immunocytochemistry

MDCK II cells were fixed with 3.0% formaldehyde in PBS for 10 min and then treated with PBS containing 0.2% Triton X-100 for 10 min. The fixed cells were blocked with 1% bovine serum albumin for 30 min and stained with the indicated antibodies. CellTracker Violet BMQC and Orange CMRA were used according to the manufacturer's protocol.

For the wound closure assay, MDCK II cells were seeded on PDL-coated 13-mm coverslips at a density of 3×10^5 cells in 35-mm dishes. After 72 h, a hole was made on the confluent cells using a 0.3-mm outer diameter sterile needle (Tochigi Seiko Co., Ltd). At 3 h after puncture, the cells were thoroughly washed with PBS and subjected to immunocytochemistry.

Coverslips were mounted with Fluoromount (Diagnostic Biosystems) and the fluorescence was examined using a confocal laser scanning microscope (LSM 780 and LSM5 PASCAL) built around an Axio Observer Z1 or Axiovert 200M with Plan Apochromat 63× (NA 1.4) and C-Apochromat 63× (NA 1.2) lenses under control of LSM software (Carl Zeiss). Images were processed using ImageJ or Photoshop (Adobe).

Statistics

Prism (GraphPad Software) was used for statistical analysis. Data were evaluated using one-way or two-way analysis of variance followed by a post-hoc Dunnett's or Sidak's multiple comparison test.

Online supplemental material

Fig. S1 shows the phosphorylation of Scrib by Rho-kinase at Ser 1378 and Ser 1508. Fig. S2 shows that Scrib associates with Shroom2 and Rho-kinase in a phosphorylation state–dependent manner. Fig. S3 shows that Scirb, Rho-kinase, and Shroom2 are accumulated and colocalized with ppMLC at the wound edges during purse string wound closure. Fig. S4 shows the Shroom2 mutants lacking the binding abilities to Scrib and Rho-kinase. Table S1 shows interactors with the C terminus of Scrib phosphorylated by Rho-kinase. Table S2 shows the list of constructs used in this study. Table S3 shows the lists of candidate phosphorylation sites detected in the screens for the indicated kinases. Online supplemental material is available at http://www.jcb.org/cgi/content/full/jcb.201412008/DC1. Additional data are available in the JCB DataViewer at http://dx.doi.org/10.1083/jcb.201412008.dv.

References

Amano, M., M. Ito, K. Kimura, Y. Fukata, K. Chihara, T. Nakano, Y. Matsuura, and K. Kaibuchi. 1996. Phosphorylation and activation of myosin by Rho-associated kinase (Rho-kinase). *J. Biol. Chem.* 271:20246–20249. http://dx.doi.org/10.1074/jbc.271.34.20246

Amano, M., K. Chihara, N. Nakamura, T. Kaneko, Y. Matsuura, and K. Kaibuchi. 1999. The COOH terminus of Rho-kinase negatively regulates rho-kinase activity. *J. Biol. Chem.* 274:32418–32424. http://dx.doi.org/10.1074/jbc.274.45.32418

Amano, M., Y. Fukata, H. Shimokawa, and K. Kaibuchi. 2000. Purification and in vitro activity of Rho-associated kinase. *Methods Enzymol.* 325:149–155.

Amano, M., M. Nakayama, and K. Kaibuchi. 2010a. Rho-kinase/ROCK: A key regulator of the cytoskeleton and cell polarity. *Cytoskeleton (Hoboken).* 67:545–554. http://dx.doi.org/10.1002/cm.20472

Amano, M., Y. Tsumura, K. Taki, H. Harada, K. Mori, T. Nishioka, K. Kato, T. Suzuki, Y. Nishioka, A. Iwamatsu, and K. Kaibuchi. 2010b. A proteomic approach for comprehensively screening substrates of protein kinases such as Rho-kinase. *PLoS ONE.* 5:e8704. http://dx.doi.org/10.1371/journal.pone.0008704

Arimura, N., and K. Kaibuchi. 2007. Neuronal polarity: from extracellular signals to intracellular mechanisms. *Nat. Rev. Neurosci.* 8:194–205. http://dx.doi.org/10.1038/nrn2056

Assémat, E., E. Bazellières, E. Pallesi-Pocachard, A. Le Bivic, and D. Massey-Harroche. 2008. Polarity complex proteins. *Biochim. Biophys. Acta.* 1778:614–630. http://dx.doi.org/10.1016/j.bbamem.2007.08.029

Audebert, S., C. Navarro, C. Nourry, S. Chasserot-Golaz, P. Lécine, Y. Bellaiche, J.L. Dupont, R.T. Premont, C. Sempéré, J.M. Strub, et al. 2004. Mammalian Scribble forms a tight complex with the βPIX exchange factor. *Curr. Biol.* 14:987–995. http://dx.doi.org/10.1016/j.cub.2004.05.051

Baines, A.J. 2010. The spectrin–ankyrin-4.1–adducin membrane skeleton: adapting eukaryotic cells to the demands of animal life. *Protoplasma.* 244:99–131. http://dx.doi.org/10.1007/s00709-010-0181-1

Biondi, R.M., and A.R. Nebreda. 2003. Signalling specificity of Ser/Thr protein kinases through docking-site-mediated interactions. *Biochem. J.* 372:1–13. http://dx.doi.org/10.1042/BJ20021641

Caddy, J., T. Wilanowski, C. Darido, S. Dworkin, S.B. Ting, Q. Zhao, G. Rank, A. Auden, S. Srivastava, T.A. Papenfuss, et al. 2010. Epidermal wound repair is regulated by the planar cell polarity signaling pathway. *Dev. Cell.* 19:138–147. http://dx.doi.org/10.1016/j.devcel.2010.06.008

Chan, P.M., and E. Manser. 2012. PAKs in human disease. *Prog. Mol. Biol. Transl. Sci.* 106:171–187.

Cohen, P. 2002. Protein kinases—the major drug targets of the twenty-first century? *Nat. Rev. Drug Discov.* 1:309–315. http://dx.doi.org/10.1038/nrd773

Cox, J., and M. Mann. 2008. MaxQuant enables high peptide identification rates, individualized p.p.b.-range mass accuracies and proteome-wide protein quantification. *Nat. Biotechnol.* 26:1367–1372. http://dx.doi.org/10.1038/nbt.1511

Dow, L.E., J.S. Kauffman, J. Caddy, K. Zarbalis, A.S. Peterson, S.M. Jane, S.M. Russell, and P.O. Humbert. 2007. The tumour-suppressor Scribble dictates cell polarity during directed epithelial migration: regulation of Rho GTPase recruitment to the leading edge. *Oncogene.* 26:2272–2282. (published erratum appears in *Oncogene.* 2007. 26:5692) http://dx.doi.org/10.1038/sj.onc.1210016

Emmert, D.A., J.A. Fee, Z.M. Goeckeler, J.M. Grojean, T. Wakatsuki, E.L. Elson, B.P. Herring, P.J. Gallagher, and R.B. Wysolmerski. 2004. Rho-kinase-mediated Ca2+-independent contraction in rat embryo fibroblasts. *Am. J. Physiol. Cell Physiol.* 286:C8–C21. http://dx.doi.org/10.1152/ajpcell.00428.2002

Endicott, J.A., M.E. Noble, and L.N. Johnson. 2012. The structural basis for control of eukaryotic protein kinases. *Annu. Rev. Biochem.* 81:587–613. http://dx.doi.org/10.1146/annurev-biochem-052410-090317

Farber, M.J., R. Rizaldy, and J.D. Hildebrand. 2011. Shroom2 regulates contractility to control endothelial morphogenesis. *Mol. Biol. Cell.* 22:795–805. http://dx.doi.org/10.1091/mbc.E10-06-0505

Fukata, Y., N. Oshiro, N. Kinoshita, Y. Kawano, Y. Matsuoka, V. Bennett, Y. Matsuura, and K. Kaibuchi. 1999. Phosphorylation of adducin by Rho-kinase plays a crucial role in cell motility. *J. Cell Biol.* 145:347–361. http://dx.doi.org/10.1083/jcb.145.2.347

Goldsmith, E.J., R. Akella, X. Min, T. Zhou, and J.M. Humphreys. 2007. Substrate and docking interactions in serine/threonine protein kinases. *Chem. Rev.* 107:5065–5081. http://dx.doi.org/10.1021/cr068221w

Gorfinkiel, N., and G.B. Blanchard. 2011. Dynamics of actomyosin contractile activity during epithelial morphogenesis. *Curr. Opin. Cell Biol.* 23:531–539. http://dx.doi.org/10.1016/j.ceb.2011.06.002

Hildebrand, J.D. 2005. Shroom regulates epithelial cell shape via the apical positioning of an actomyosin network. *J. Cell Sci.* 118:5191–5203. http://dx.doi.org/10.1242/jcs.02626

Hodgson, D.R., and M. Schröder. 2011. Chemical approaches towards unravelling kinase-mediated signalling pathways. *Chem. Soc. Rev.* 40:1211–1223. http://dx.doi.org/10.1039/C0CS00020E

Hornbeck, P.V., J.M. Kornhauser, S. Tkachev, B. Zhang, E. Skrzypek, B. Murray, V. Latham, and M. Sullivan. 2012. PhosphoSitePlus: a comprehensive resource for investigating the structure and function of experimentally determined post-translational modifications in man and mouse. *Nucleic Acids Res.* 40:D261–D270. http://dx.doi.org/10.1093/nar/gkr1122

Humbert, P.O., N.A. Grzeschik, A.M. Brumby, R. Galea, I. Elsum, and H.E. Richardson. 2008. Control of tumourigenesis by the Scribble/Dlg/Lgl polarity module. *Oncogene.* 27:6888–6907. http://dx.doi.org/10.1038/onc.2008.341

Kaibuchi, K., S. Kuroda, and M. Amano. 1999. Regulation of the cytoskeleton and cell adhesion by the Rho family GTPases in mammalian cells. *Annu. Rev. Biochem.* 68:459–486. http://dx.doi.org/10.1146/annurev.biochem.68.1.459

Karnak, D., S. Lee, and B. Margolis. 2002. Identification of multiple binding partners for the amino-terminal domain of synapse-associated protein 97. *J. Biol. Chem.* 277:46730–46735. http://dx.doi.org/10.1074/jbc.M208781200

Keicher, C., S. Gambaryan, E. Schulze, K. Marcus, H.E. Meyer, and E. Butt. 2004. Phosphorylation of mouse LASP-1 on threonine 156 by cAMP- and cGMP-dependent protein kinase. *Biochem. Biophys. Res. Commun.* 324:308–316. http://dx.doi.org/10.1016/j.bbrc.2004.08.235

Kimura, K., M. Ito, M. Amano, K. Chihara, Y. Fukata, M. Nakafuku, B. Yamamori, J. Feng, T. Nakano, K. Okawa, et al. 1996. Regulation of myosin phosphatase by Rho and Rho-associated kinase (Rho-kinase). *Science.* 273:245–248. http://dx.doi.org/10.1126/science.273.5272.245

Kimura, K., Y. Fukata, Y. Matsuoka, V. Bennett, Y. Matsuura, K. Okawa, A. Iwamatsu, and K. Kaibuchi. 1998. Regulation of the association of adducin with actin filaments by Rho-associated kinase (Rho-kinase) and myosin phosphatase. *J. Biol. Chem.* 273:5542–5548. http://dx.doi.org/10.1074/jbc.273.10.5542

Kondoh, K., and E. Nishida. 2007. Regulation of MAP kinases by MAP kinase phosphatases. *Biochim. Biophys. Acta.* 1773:1227–1237. http://dx.doi.org/10.1016/j.bbamcr.2006.12.002

Lee, C., M.P. Le, and J.B. Wallingford. 2009. The shroom family proteins play broad roles in the morphogenesis of thickened epithelial sheets. *Dev. Dyn.* 238:1480–1491. http://dx.doi.org/10.1002/dvdy.21942

Mammoto, T., and D.E. Ingber. 2010. Mechanical control of tissue and organ development. *Development.* 137:1407–1420. http://dx.doi.org/10.1242/dev.024166

Mizushima, S., and S. Nagata. 1990. pEF-BOS, a powerful mammalian expression vector. *Nucleic Acids Res.* 18:5322. http://dx.doi.org/10.1093/nar/18.17.5322

Montcouquiol, M., R.A. Rachel, P.J. Lanford, N.G. Copeland, N.A. Jenkins, and M.W. Kelley. 2003. Identification of Vangl2 and Scrb1 as planar polarity genes in mammals. *Nature.* 423:173–177. http://dx.doi.org/10.1038/nature01618

Murdoch, J.N., D.J. Henderson, K. Doudney, C. Gaston-Massuet, H.M. Phillips, C. Paternotte, R. Arkell, P. Stanier, and A.J. Copp. 2003. Disruption of scribble (Scrb1) causes severe neural tube defects in the circletail mouse. *Hum. Mol. Genet.* 12:87–98. http://dx.doi.org/10.1093/hmg/ddg014

Nakayama, M., T.M. Goto, M. Sugimoto, T. Nishimura, T. Shinagawa, S. Ohno, M. Amano, and K. Kaibuchi. 2008. Rho-kinase phosphorylates PAR-3 and disrupts PAR complex formation. *Dev. Cell.* 14:205–215. http://dx.doi.org/10.1016/j.devcel.2007.11.021

Namba, T., Y. Kibe, Y. Funahashi, S. Nakamuta, T. Takano, T. Ueno, A. Shimada, S. Kozawa, M. Okamoto, Y. Shimoda, et al. 2014. Pioneering axons regulate neuronal polarization in the developing cerebral cortex. *Neuron.* 81:814–829. http://dx.doi.org/10.1016/j.neuron.2013.12.015

Nishimura, T., and M. Takeichi. 2008. Shroom3-mediated recruitment of Rho kinases to the apical cell junctions regulates epithelial and neuroepithelial planar remodeling. *Development.* 135:1493–1502. http://dx.doi.org/10.1242/dev.019646

Palmeri, A., F. Ferrè, and M. Helmer-Citterich. 2014. Exploiting holistic approaches to model specificity in protein phosphorylation. *Front. Genet.* 5:315. http://dx.doi.org/10.3389/fgene.2014.00315

Patwari, P., and R.T. Lee. 2008. Mechanical control of tissue morphogenesis. *Circ. Res.* 103:234–243. http://dx.doi.org/10.1161/CIRCRESAHA.108.175331

Peng, J., J.E. Elias, C.C. Thoreen, L.J. Licklider, and S.P. Gygi. 2003. Evaluation of multidimensional chromatography coupled with tandem mass spectrometry (LC/LC-MS/MS) for large-scale protein analysis: the yeast proteome. *J. Proteome Res.* 2:43–50. http://dx.doi.org/10.1021/pr025556v

Peti, W., and R. Page. 2013. Molecular basis of MAP kinase regulation. *Protein Sci.* 22:1698–1710. http://dx.doi.org/10.1002/pro.2374

Petit, M.M., S.M. Meulemans, P. Alen, T.A. Ayoubi, E. Jansen, and W.J. Van de Ven. 2005. The tumor suppressor Scrib interacts with the zyxin-related protein LPP, which shuttles between cell adhesion sites and the nucleus. *BMC Cell Biol.* 6:1. http://dx.doi.org/10.1186/1471-2121-6-1

Phillips, H.M., H.J. Rhee, J.N. Murdoch, V. Hildreth, J.D. Peat, R.H. Anderson, A.J. Copp, B. Chaudhry, and D.J. Henderson. 2007. Disruption of planar cell polarity signaling results in congenital heart defects and cardiomyopathy attributable to early cardiomyocyte disorganization. *Circ. Res.* 101:137–145. http://dx.doi.org/10.1161/CIRCRESAHA.106.142406

Riento, K., and A.J. Ridley. 2003. Rocks: multifunctional kinases in cell behaviour. *Nat. Rev. Mol. Cell Biol.* 4:446–456. http://dx.doi.org/10.1038/nrm1128

Simons, M., and M. Mlodzik. 2008. Planar cell polarity signaling: from fly development to human disease. *Annu. Rev. Genet.* 42:517–540. http://dx.doi.org/10.1146/annurev.genet.42.110807.091432

Taylor, S.S., R. Ilouz, P. Zhang, and A.P. Kornev. 2012. Assembly of allosteric macromolecular switches: lessons from PKA. *Nat. Rev. Mol. Cell Biol.* 13:646–658. http://dx.doi.org/10.1038/nrm3432

Walsh, M.P. 2011. Vascular smooth muscle myosin light chain diphosphorylation: mechanism, function, and pathological implications. *IUBMB Life.* 63:987–1000. http://dx.doi.org/10.1002/iub.527

Wansleeben, C., and F. Meijlink. 2011. The planar cell polarity pathway in vertebrate development. *Dev. Dyn.* 240:616–626. http://dx.doi.org/10.1002/dvdy.22564

Yamaguchi, H., M. Kasa, M. Amano, K. Kaibuchi, and T. Hakoshima. 2006. Molecular mechanism for the regulation of rho-kinase by dimerization and its inhibition by fasudil. *Structure.* 14:589–600. http://dx.doi.org/10.1016/j.str.2005.11.024

Yoshihara, K., J. Ikenouchi, Y. Izumi, M. Akashi, S. Tsukita, and M. Furuse. 2011. Phosphorylation state regulates the localization of Scribble at adherens junctions and its association with E-cadherin–catenin complexes. *Exp. Cell Res.* 317:413–422. http://dx.doi.org/10.1016/j.yexcr.2010.12.004